

# An ensemble estimate of Australian soil organic carbon using machine learning and process-based modelling

Lingfei Wang<sup>1,2</sup>, Gab Abramowitz<sup>1,2</sup>, Ying-Ping Wang<sup>3</sup>, Andy Pitman<sup>1,2</sup> and Raphael A. Viscarra Rossel<sup>4</sup>

<sup>1</sup> ARC Center of Excellence for Climate Extremes, Sydney NSW 2052, Australia

<sup>2</sup> Climate Change Research Center, University of New South Wales, Sydney NSW 2052, Australia

<sup>3</sup> CSIRO Environment, Private Bag 10, Clayton South VIC 3169, Australia

<sup>4</sup> Soil & Landscape Science, School of Molecular & Life Sciences, Faculty of Science & Engineering, Curtin University, GPO Box U1987, Perth WA 6845, Australia.

Correspondence to: Lingfei Wang ([lingfei.wang@unsw.edu.au](mailto:lingfei.wang@unsw.edu.au))

## Abstract

Spatially explicit prediction of soil organic carbon (SOC) serves as a crucial foundation for effective land management strategies aimed at mitigating soil degradation and assessing carbon sequestration potential. Here, using more than 1000 in-situ observations, we trained two machine learning models (random forest, and K-means coupled with multiple linear regression), and one process-based model (the vertically resolved Microbial-MIneral Carbon Stabilization (MIMICS)) to predict SOC stocks of the top 30 cm of soil in Australia. Parameters of MIMICS were optimized for different site groupings, using two distinct approaches, plant functional types (MIMICS-PFT), and the most influential environmental factors (MIMICS-ENV). All models showed good performance in SOC predictions with  $R^2$  greater than 0.8 during out-of-sample validation with random forest being the most accurate, and SOC in forests is more predictable than that in non-forest soils excluding croplands. The performance of continental-scale SOC predictions by MIMICS-ENV is better than that by MIMICS-PFT especially in non-forest soils. Digital maps of terrestrial SOC stocks generated using all the models showed similar spatial distribution with higher values in southeast and southwest Australia, but the magnitude of estimated SOC stocks varied. The mean ensemble estimate of SOC stocks was  $30.3 \text{ t ha}^{-1}$  with K-means coupled with multiple linear regression generating the highest estimate (mean SOC stocks at  $38.15 \text{ t ha}^{-1}$ ) and MIMICS-PFT generating the lowest estimate (mean SOC stocks at  $24.29 \text{ t ha}^{-1}$ ). We suggest that enhancing process-based models to incorporate newly identified drivers that significantly influence SOC variations in different environments could be key to reducing the discrepancies in these estimates. Our findings underscore the considerable uncertainty in SOC estimates derived from different modelling approaches and emphasize the importance of rigorous out-of-sample validation before applying any one approach in Australia.

Deleted: content

Deleted: We found that at the continental scale, soil bulk density and mean annual temperature are the dominant controls of SOC variation, and that dominant controls vary for different vegetation types.

Deleted: Parameter optimization approaches made a notable difference in the performance

Deleted: of MIMICS

Deleted: prediction with

Deleted: performing

Deleted: 08

Deleted: t/ha

Deleted: t/ha

Formatted: Superscript

Deleted: t/ha

## 1. Introduction

Globally, the soil is the largest biogeochemically active terrestrial carbon pool, storing more organic carbon than plants and the atmosphere combined (Jackson et al., 2017). The turnover of soil organic carbon (SOC) is a key function in plant growth, maintenance of soil water and nutrients, soil structure stabilization and other biogeochemical processes (Lefèvre et al., 2017). Soil can act as either a carbon sink or carbon source depending on the balance of carbon input through plant litter and root exudates and output through respiration and leaching (Terrer et al., 2021; Panchal et al., 2022). Even a small change in SOC stocks, in any direction, could significantly affect the atmospheric concentration of CO<sub>2</sub> and thereby climate change (Stockmann et al., 2013).

Given the importance of SOC, there is now a large and growing interest in estimating spatially explicit SOC content and stocks. SOC supports critically important soil-derived ecosystem services, and the amount of SOC indicates the degree of land and soil degradation (Lorenz et al., 2019). SOC content below a certain limit will lead to the decline of microbial diversity, water holding capacity and soil productivity (Stockmann et al., 2015). Additionally, with growing concerns about increasing anthropogenic CO<sub>2</sub> emissions, soil carbon sequestration has emerged as a potential strategy for climate change mitigation (Smith, 2016; Rumpel et al., 2018). Protection of existing SOC and rebuilding depleted stocks through land management are potential strategies in mitigating climate change (Bossio et al., 2020). However, effective SOC management requires accurate knowledge of its existing distribution. Reliable estimates of SOC stocks and their spatial variation serve as a reference point for assessing how close soil is to its maximum SOC storage capacity and its potential to sequester additional carbon (Six et al., 2002; Georgiou et al., 2022). Precise estimation of contemporary SOC stocks also provides a baseline map that can be used to calibrate and initialize dynamic-mechanistic models, enabling the study of how SOC will respond to climate and land-use change (Minasny et al., 2013; Viscarra Rossel et al., 2014). It is, for example, a prerequisite for accurately predicting future carbon–climate ~~feedback~~ in Earth system models (ESMs) (Todd-Brown et al., 2013).

Deleted: feedbacks

Accurately assessing SOC storage is challenging due to the complexity of carbon formation and degradation processes in space and time (Keskin et al., 2019). Soil exists as a continuum containing organic compounds at different stages of decomposition (Lehmann and Kleber, 2015). Soil formation can be described by a function of climate, organisms, relief, parent material and time (Jenny, 1941). These factors are widely used in SOC studies for digital soil mapping (McBratney et al., 2003; Viscarra Rossel et al., 2015; Liang et al., 2019). However, the relationship between SOC storage and these driving variables is complex and spatially variable (Mishra and Riley, 2015; Viscarra Rossel et al., 2019; Adhikari et al., 2020) leading to substantial challenges and inherent uncertainties in SOC predictions.

Deleted: 1994

Mechanistic process-based models and empirical models (including machine learning models) are two widely employed approaches used to predict SOC stocks and their spatial distribution.

99 Conventional process-based models assume first-order kinetics for SOC decomposition,  
100 wherein the rate of C decomposition is dependent on temperature and moisture but independent  
101 of microbial biomass, and equilibrium SOC stock is proportional to carbon input and mean  
102 residence time (Abs and Ferrière, 2020; Wang et al., 2021). ESMS coupled with conventional  
103 SOC models cannot accurately ~~simulate spatial pattern~~ of contemporary soil carbon and show  
104 ~~large divergence~~ in projected SOC dynamics under future climate change (Todd-Brown et al.,  
105 2013; Todd-Brown et al., 2014). ~~In addition to the biases introduced by errors in model  
106 parameters and the lack of independent model validation based on observed time series data,  
107 the uncertainties in predicted SOC by ESMS can also result from~~ the lack of explicit  
108 representation of soil microbial activities and metabolic traits (Wieder et al., 2015; Le Neo et  
109 al., 2023). Numerous microbial models have been developed in the past few decades to improve  
110 model performance of SOC predictions (Chandel et al., 2023), but these models ~~have~~ rarely  
111 been incorporated into large-scale modelling frameworks ~~due to the difficulty of constraining  
112 parameters relating to microbial activities and~~ the lack of rigorous validation (Todd-Brown et  
113 al., 2013; Luo et al., 2016). Process-based SOC models are constructed based on our  
114 understanding ~~of~~ the major processes governing SOC dynamics (e.g., carbon input,  
115 decomposition, and loss). However, the disagreement in projections of carbon dynamics by  
116 different models highlights the need to improve our knowledge of SOC cycling (Luo et al.,  
117 2016). Machine learning models without any process-level assumptions provide a tool to  
118 identify the most influential controls on SOC variations. Machine learning models can represent  
119 non-linear and non-smooth relationships between predictor and response variables as well as  
120 interactions between different predictors (Heung et al., 2016). Various machine learning  
121 algorithms have been successfully used in digital soil mapping to predict high-resolution  
122 spatially explicit SOC ~~concentration/stocks~~ (Lamichhane et al., 2019).

123  
124 Several modelling studies of soil carbon ~~stocks~~ have been conducted in Australia. Wang et al.  
125 (2018a) trained boosted regression trees and random forest models using ~~field observations and~~  
126 ~~applied the trained random forest model~~ to map the spatial distribution of SOC at two soil depths  
127 (0-5 cm and 0-30 cm) ~~for the semi-arid rangelands of eastern Australia~~. Continentally, Viscarra  
128 Rossel et al. (2014) trained the CUBIST model, a form of piecewise linear decision tree, using  
129 more than five thousand observations to produce a high resolution (90 m × 90 m) baseline map  
130 of SOC stocks of Australian terrestrial systems and its uncertainty ~~of the top 30 cm soils~~. Based  
131 on the baseline map, Walden et al. (2023) derived spatially explicit estimates of Australian SOC  
132 stocks and uncertainty including additional data from forests from southeastern Australia and  
133 coastal marine (or blue carbon) ecosystems. SOC content at multiple soil depths along with  
134 associated uncertainties were also estimated using different machine learning algorithms  
135 (Viscarra Rossel et al., 2015; Wadoux et al., 2023). Moreover, the distribution of different soil  
136 carbon compositions (i.e., the particulate, mineral-associated and pyrogenic organic carbon  
137 fractions) and the importance of environmental factors on their variations were also studied  
138 using machine learning (Viscarra Rossel et al., 2019). However, despite the progress made in  
139 SOC modelling, significant uncertainties persist in SOC estimates due to the inherent  
140 complexities of SOC variations ~~and~~ the lack of appropriately sampled SOC observations. All

Deleted: predict

Deleted: s

Deleted: high uncertainties

Deleted: This is partly due to

Deleted: s

Deleted: partly

Deleted: .

Deleted: on

Deleted: content

Deleted: content/

Deleted: from the semi-arid rangelands of eastern Australia. Both models predicted SOC stocks moderately well based on performance metrics. The

Deleted: fitted model

Deleted: s

Deleted: were then applied

Deleted: at 30 cm depth

Deleted: .

Deleted: and the amount of data

160 these continental estimates were generated using empirical modelling approaches or first-order  
161 biogeochemical models without explicitly representing the important role of soil microbes in  
162 SOC stabilization (Grace et al., 2006; Lee et al., 2021). Estimates from mechanistic SOC  
163 models with explicit representation of microbial metabolism are missing despite offering the  
164 potential to better constrain SOC dynamics under future climate change scenarios in a way that  
165 empirical approaches cannot.

166  
167 Our primary objective in this paper is to assess the predictability of SOC concentration,  
168 (excluding cropland soils) in Australia and generate a range of estimates of terrestrial SOC  
169 stocks, employing both process-based and empirical modelling, and examine why these  
170 estimates might differ. First, we discern the significance of environmental predictors, both at  
171 continental and biome scales. We then evaluate the performance of random forests, K-means  
172 with multiple linear regression and the vertically resolved MIMICS model with different  
173 parametrization approaches. Finally, we compare the spatial estimates of SOC stocks using  
174 these different approaches across Australia, and discuss their differences and potential  
175 application to future SOC projection.

176

## 177 2. Materials and Methods

### 178 2.1. Model descriptions

#### 179 2.1.1. Vertically resolved MIMICS

180  
181 The MIMICS model (Wieder et al., 2015; Zhang et al., 2020) explicitly considers relationships  
182 between litter quality, functional trade-offs in microbial physiology, and the physical protection  
183 of microbial by-products in forming stable soil organic matter. There are two litter pools:  
184 metabolic ( $LIT_m$ ) and structural ( $LIT_s$ ) litter (Figure 1), and the partitioning of litter input into  
185 metabolic and structural pools is determined by the chemical properties of the litter. Litter and  
186 SOC turnover are governed by two microbial functional types that exhibit copiotrophic (i.e., r-  
187 selected,  $MIC_r$ ) and oligotrophic (i.e., K-selected,  $MIC_k$ ) growth strategies. The  $MIC_r$  is  
188 assumed to have higher growth and turnover rates, and a preference for consuming labile litter  
189 ( $LIT_m$ ), while  $MIC_k$  is characterized by lower growth and turnover rates, and a greater  
190 competitive advantage when consuming low-quality litter ( $LIT_s$ ) and chemically recalcitrant  
191 SOC. SOC in MIMICS is divided into three pools: physically protected ( $SOC_p$ ),  
192 (bio)chemically recalcitrant ( $SOC_c$ ) and available ( $SOC_a$ ) carbon (Figure 1).

193

Deleted: stocks

Deleted: .

Deleted: We

Deleted: k

Deleted: Microbial-MIneral Carbon Stabilization (

Deleted: )

Deleted: SOC

Deleted: Microbial-MIneral Carbon Stabilization (

Deleted: )

Deleted: is a soil carbon model that

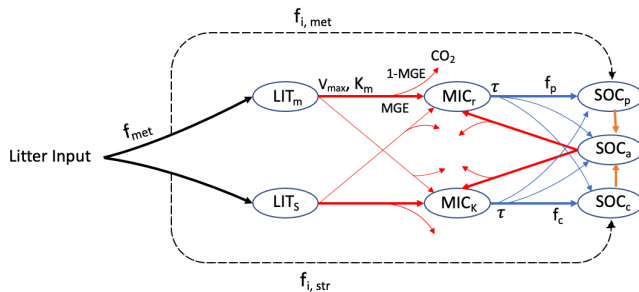


**Figure 1.** SOC pools and fluxes represented in MIMICS (adapted from Wieder et al., (2015)). Litter inputs are partitioned into metabolic and structural litter pools (LIT<sub>m</sub> and LIT<sub>s</sub>) based on litter quality (f<sub>i,met</sub>). Decomposition of litter and available SOC pool (SOC<sub>a</sub>) are governed by temperature sensitive Michaelis-Menten kinetics (V<sub>max</sub> (maximum reaction velocity) and K<sub>m</sub> (half saturation constant)), shown by red lines. Microbial growth efficiency (MGE) determines the partitioning of C fluxes entering microbial biomass pools vs. heterotrophic respiration. Turnover of microbial biomass (τ, blue) depends on microbial functional types (MIC<sub>r</sub> and MIC<sub>k</sub>), and is partitioned into available, physically protected and chemically recalcitrant SOC pools (SOC<sub>a</sub>, SOC<sub>p</sub> and SOC<sub>c</sub>, respectively).

The decomposition of litter pools and SOC pools follows temperature-sensitive Michaelis-Menten kinetics. Microbial growth efficiency (MGE) determines the partitioning of carbon fluxes entering microbial biomass pools (MIC<sub>r</sub> and MIC<sub>k</sub>) versus heterotrophic respiration. Access of microbial enzymes to available substrates depends on soil texture. The equations of MIMICS are from Wieder et al. (2015), except that the density-dependent microbial turnover was introduced to MIMICS to minimize an unrealistic oscillation (Zhang et al., 2020). To better simulate carbon turnover at different soil depths, vertical transport of soil carbon was introduced into MIMICS considering carbon transported through bioturbation and diffusion among adjacent soil layers (Wang et al., 2021).

Vertically resolved MIMICS is run using a daily time step. The soil was divided into 15 layers, each of 10 cm thickness. All the sites in this study are assumed to be at steady state (i.e., no interannual variation of SOC). Historical climate, litterfall input and soil properties were all assumed to be similar to the average conditions. At each site, the initial pool fractions were 0.03, 0.03, 0.14, 0.47 and 0.33 for MIC<sub>r</sub>, MIC<sub>k</sub>, SOC<sub>p</sub>, SOC<sub>c</sub> and SOC<sub>a</sub>, respectively. All pools were then spun up to finally achieve steady state with the maximal difference in any pool size between two successive spins being less than 0.05%.

### 2.1.2. Machine learning

Two machine learning algorithms were applied in this study to predict SOC. First, random forest (RF) is a tree-based ensemble learning method that works by building a set of regression trees and averaging results (Breiman, 2001). Within the training procedure, the RF algorithm produces multiple trees. Each regression tree in the forest is independently constructed based on a unique bootstrap sample (with replacement) from the original training data set. The

Deleted: Soil carbon

Deleted: is restricted

Deleted: by

Deleted: the

Deleted: pool size was initialized within a sensible range

Formatted: Subscript

Formatted: Subscript

Formatted: Subscript

Formatted: Subscript

Formatted: Subscript

Deleted: for different pools and

245 response, as well as the predictor variables are either categorical (classification trees) or  
246 numeric (regression trees). Bootstrap sampling makes RF less sensitive to overfitting and  
247 allows for robust error estimation based on the remaining test set, the so-called Out-Of-Bag  
248 (OOB) sample (Wiesmeier et al., 2014). We used the “ranger” package R (version 4.2.0) for RF  
249 computation. We trained the RF model with different numbers (100, 200, 300, 400 and 500) of  
250 trees and observed that the model's performance remained similar regardless of the number of  
251 trees used. The number of regression trees generated in the forest (num.trees) was finally set as  
252 200, and the number of predictors randomly selected at each node (mtry) was set as default,  
253 which was 2.

254  
255 Multiple linear regression (MLR) is widely used in SOC studies but found to be less effective  
256 than machine learning algorithms (Lamichhane et al., 2019). Here, instead of applying MLR  
257 directly with all environmental factors as predictors, our approach involved a preliminary step  
258 where we partitioned all observations into distinct clusters using K-means, an unsupervised  
259 machine learning algorithm. K-means aims to divide the data into a predefined number of  
260 clusters (k), with the objective of maximizing the similarity among data within each cluster.  
261 The underlying assumption here was that sites sharing similar environmental conditions would  
262 exhibit comparable SOC concentration. In cases where certain clusters had fewer observations  
263 than five times the number of predictors, we augmented these clusters by incorporating  
264 observations from other clusters. This augmentation process was guided by the Euclidean  
265 distance between the observation and the cluster centre, ensuring a more robust construction of  
266 the linear regression model. To determine the number of clusters, we applied the coupled K-  
267 means and MLR with varying number of clusters. The selection of the optimal number of  
268 clusters was based on the criterion of producing the smallest root mean square error during  
269 independent out-of-sample validation.

## 270 271 2.2. Relative importance of environmental variables for SOC prediction

272  
273 RF-based measures of variable importance have gained widespread popularity as tools for  
274 evaluating the contributions made by predictor variables within a fitted random forest model  
275 (Debeer and Strobl, 2020). In the context of this study, we employed permutation variable  
276 importance (PVI) within the random forest framework to gauge the significance of predictors  
277 (see Section 2.4) in predicting SOC concentration.

278  
279 The PVI entails measuring the reduction in a RF model's performance score upon random  
280 shuffling of a single variable values. By doing so, the inherent relationship between the variable  
281 and the SOC concentration is disrupted. Consequently, the disparity in prediction accuracy  
282 observed in a RF model before and after such shuffling serves as a quantitative representation  
283 of the significance of the particular predictor in predicting SOC concentration. The greater the  
284 importance of the predictor, the higher its corresponding PVI value becomes.

Deleted: segregate

Deleted: Identification of dominant controllers on SOC concentration

Deleted: permutation variable importance

Deleted: random forest

292 2.3. Parameter optimization

293  
294 MIMICS parameters were derived from Zhang et al., (2020) and Wang et al., (2021), except that  
295 five parameters (Table 1) which directly control the organic carbon decomposition were  
296 optimized. An effective global optimization algorithm called the shuffled complex evolution  
297 (SCE-UA, version 2.2) method (Duan et al., 1993) was applied for parameter optimization, by  
298 minimizing the sum of squared residuals between the observed and modelled values.

- Deleted: (
- Deleted: ,
- Deleted: ;
- Deleted: ,
- Deleted: . Parameters were optimized

299  
300 Vertically resolved MIMICS simulated SOC concentration for 15 soil layers with a uniform  
301 layer thickness of 10 cm. As observations only provide one measurement for the top 30 cm soil,  
302 we computed the average of the modelled values spanning the 0-10 cm, 10-20 cm, and 20-30  
303 cm soil layers. This average was then adopted as the modelled SOC concentration for top 30  
304 cm soil, serving as the basis for evaluating the difference between observations and simulations.

305  
306 **Table 1.** The optimized model parameters (dimensionless) and their value range.

Parameter	Definition	Range
$a_v$	A scaling factor for $V_{max}$	0-30
$a_k$	A scaling factor for $K_m$	0-20
xdesorp	A scaling factor for SOC desorption rate	0-3
xbeta	An exponent of the biomass density dependent mortality rate of microbes	1.05-2
xdiffsoc	A scaling factor for SOC diffusion coefficient in soil	0-30

307  
308 Parameters in MIMICS were optimized for different groups divided based on two approaches.  
309 The first approach involved categorizing all observations into four groups based on plant  
310 functional type (PFT). The second approach used the most influential abiotic variables as  
311 predictors (as outlined in Section 2.2) and divided all observations into 6 clusters using the K-  
312 means algorithm. The determination of the optimal number of clusters was achieved through  
313 the minimization of the sum of the within-cluster-sum-of-squares-of-all-clusters (WCSSE), a  
314 process facilitated by the "ClusterR" package in R (version 4.2.0). This clustering aimed to  
315 ensure the highest possible similarity among the environmental factors within each cluster. It  
316 was anticipated that SOC ranges within each cluster would be narrow due to the high similarity  
317 of environmental predictors.

- Deleted: distinct
- Deleted: s
- Deleted: s
- Deleted: was
- Deleted: taking
- Deleted: dividing

318  
319 2.4. Data

320 2.4.1. Predictors of spatial variations of observed SOC concentration.

321  
322 MIMICS requires gridded mean annual temperature (MAT), carbon input and clay content as  
323 driving variables for a spatial simulation. Gridded mean annual precipitation (MAP) and  
324 vegetation types were also used during calibration and when understanding the drivers and  
325 spatial variability of SOC. Details of gridded data can be found in Table 2.

- Deleted: concentration
- Deleted: Soil bulk density
- Deleted: is also required for conversion between SOC concentration (g C/kg soil) and SOC stocks (t/ha).

326  
327 Gridded daily maximum temperature, minimum temperature, and precipitation at 0.05°  
328 resolution were obtained from the SILO database (Jeffrey et al., 2001) of Australian climate  
329 data. Mean daily temperature was approximated as the average of maximum and minimum

345 daily temperature. MAT was calculated from mean daily temperature from 1991 to 2020, and  
346 MAP was calculated from daily precipitation from 1991 to 2020.

347  
348 Carbon input was represented by NPP. Gridded mean annual NPP at 500 m was calculated  
349 based on annual NPP from 2001 to 2020 obtained from MODIS (MOD17A3HGF V6.1)  
350 (Running and Zhao, 2021). NPP was partitioned to above-/belowground part by multiplying by  
351 the root/shoot ratio for different vegetation types (Mokany et al., 2006). Here we did not account  
352 for the fraction of NPP that is appropriated by human activities.

353  
354 The distribution of vegetation types at 3'' resolution was obtained from National Vegetation  
355 Information System (NVIS, version 6.0, [https://www.dccceew.gov.au/environment/land/native-](https://www.dccceew.gov.au/environment/land/native-vegetation/national-vegetation-information-system)  
356 [vegetation/national-vegetation-information-system](https://www.dccceew.gov.au/environment/land/native-vegetation/national-vegetation-information-system)). Pixels of non-vegetated regions were  
357 removed and 28 types from NVIS were aggregated to just 4 PFT; forest, woodland, shrubland  
358 and grassland.

359  
360 Soil bulk density and clay content were obtained from Soil and Landscape Grid National Soil  
361 Attributes Maps (SLGA – Release 2) (Grundy et al., 2015; Viscarra Rossel et al., 2015). Soil  
362 properties were predicted based on machine learning at depths 0-5 cm, 5-15 cm, 15-30 cm, 30-  
363 60 cm, 60-100 cm, and 100-200 cm in SLGA. Bulk density and clay content were estimated for  
364 top 30 cm soil as weighted average of first 3 layers in SLGA.

365  
366 The initial spatial resolution of the gridded data was maintained when extracting the required  
367 environmental factors for each SOC observation. All data were then resampled to 0.05°  
368 resolution using bilinear interpolation for estimation of terrestrial SOC stocks at continental  
369 scale.

370  
371 **Table 2.** Information of gridded data used in this study.

	Source	Spatial Scale	Temporal Scale	Unit	Time Period
Maximum Temperature	SILO	~5 km	daily	°C	1991-2020
Minimum Temperature	SILO	~5 km	daily	°C	1991-2020
Precipitation	SILO	~5 km	daily	mm	1991-2020
NPP	MODIS	500 m	annually	g C/m <sup>2</sup> /year	2001-2020
Vegetation Types	NVIS	100 m	/	/	/
Soil Bulk Density	SLGA	~90 m	/	kg/m <sup>3</sup>	/
Soil Clay Content	SLGA	~90 m	/	%	/

372  
373 2.4.2. Soil organic carbon observations

374  
375 SOC observations for top 30 cm soil in Australia were collected from two datasets. The first  
376 dataset is described in Viscarra Rossel et al. (2014) and Viscarra Rossel et al. (2019). We  
377 removed the observations collected from croplands based on the land-use record in the dataset  
378 and removed those from unvegetated regions based on NVIS vegetation map (see above). A  
379 total of 1070 site observations with only 38 from forest soils were retained. SOC stocks were  
380 reported in t ha<sup>-1</sup>. To better represent SOC distribution in forest, we obtained additional forest  
381 SOC observations from a second dataset, the Biomes of Australian Soil Environments (BASE)

Deleted: s

Formatted Table

Formatted: Not Superscript/ Subscript

Deleted: one,

Deleted: VR dataset,

Deleted: (

Deleted: ,

Deleted: ;

Deleted: ,

Deleted: Observations at

Deleted: sites

Deleted: remained.



described in Bissett et al. (2016). Here, SOC (%) was reported for 0-10 and 20-30 cm. We estimated SOC for 0-30 cm soil following the method described in Viscarra Rossel et al. (2014).

To compare the observations with MIMICS outputs, we then converted both simulated SOC (mg/cm<sup>3</sup>) and observed SOC (t/ha) in the first dataset (Viscarra Rossel et al. 2014) to SOC concentration (g C/kg soil) using spatially explicit soil bulk density (BD) from SLGA. The unit conversion will not affect the results of MIMICS. Soil clay content is extracted from SLGA.

The spatial distribution of SOC observations from different PFT is shown in Figure 2a. SOC concentration in top 30 cm is positively skewed, ranging from 1.36 to 59.73 g C/kg soil with mean value at 9.97 g C/kg soil and median value at 6.11 g C/kg soil. SOC concentration in grassland, shrubland and woodland show similar distribution patterns (Figure 2b), while SOC concentration in forest is more variable with a standard deviation at 15.92 g C/kg soil.

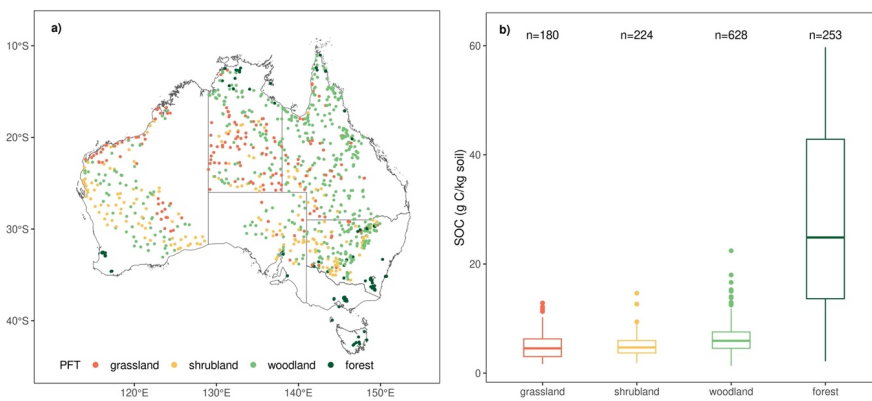


**Figure 2.** a) Spatial distribution of 1285 soil organic carbon observations used in this study and the plant functional types which they belong to; b) boxplots of SOC concentration distributions for each plant functional type. For boxplots, centre lines represent the median value, and upper and lower box boundaries represent third and first quartile. Whiskers extend to the smallest and largest values within 1.5 times the interquartile range.

## 2.5. Model evaluation

For machine learning models, 70% of the observations were randomly selected as training data to train the models and the remaining 30% used as test data to validate the predictions of SOC concentration. For vertically resolved MIMICS, parameters were optimized for each PFT or environmental group (see Section 2.3 above), and we again randomly selected 70% of

Deleted: t/ha and converted to SOC concentration (g C/kg soil) using soil bulk density (BD, kg/m<sup>3</sup>) and soil depth (m).

$$SOC_{concentration} = \frac{SOC_{stock}}{(BD \times depth) \times 100} \quad (1)$$

Clay content and soil bulk density were reported in this dataset and also in Viscarra Rossel et al. (2015). To better represent SOC distribution in forest, we obtained more forest SOC observations from a second dataset, the Biomes of Australian Soil Environments (BASE) described in (Bissett et al., 2016). Here, SOC concentration was reported for 0-10 and 20-30 cm, and we estimated the SOC concentration for 20-30 cm soil using the algorithm (Jobbágy and Jackson, 2000) below.

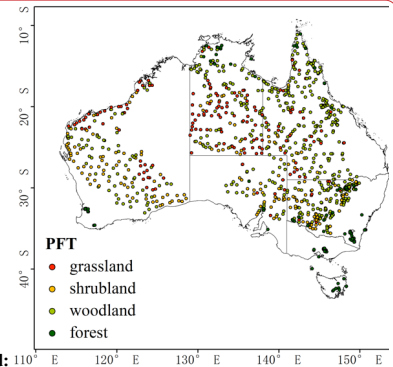
$$S \log_{10} d + I \quad \log_{10} C = \quad (2)$$

Where  $C$  represents the SOC stocks (t/ha), and  $d$  represents depth.  $S$  and  $I$  are parameters of the model.

Formatted: Font:

Deleted: We took the average SOC concentration of three layers as the value for top 30 cm soil. Clay content was reported in this dataset and bulk density was extracted from SLGA (see above).

Deleted: s



Deleted: 110° E 120° E 130° E 140° E 150° E

Deleted: concentration

Deleted: (a)

Deleted: (b)

Deleted: all

Deleted: separated to a

Deleted: test dataset randomly with 70% used to train the model and ...

Deleted: used

Deleted: group

459 observations in each group to train the model and used the remaining 30% for validation. To  
460 cross-validate, the procedure was repeated 10 times.

461  
462 The performance of models was evaluated using four metrics. Mean Absolute Error (MAE)  
463 indicates how close the average predictions are to average observations. Root Mean Square  
464 Error (RMSE) measures the overall accuracy combining mean, standard deviation differences  
465 (across sites) and (spatial) correlation. Coefficient of determination ( $R^2$ ) measures the  
466 percentage of variation explained by the model. Lin's Concordance Correlation Coefficient  
467 (LCCC) (Lawrence and Lin, 1989) measures the level of agreement between predictions and  
468 observations following the 1:1 line. A good model will have MAE and RMSE close to 0 and  $R^2$   
469 and LCCC close to 1.

## 470 2.6. Estimation of terrestrial SOC stocks

471  
472 SOC concentrations were used to train the models, and we then estimated terrestrial SOC stocks  
473 and their continental-scale spatial distribution in top 30 cm soil utilizing the four models  
474 validated within this study. SOC stock ( $t\ ha^{-1}$ ) is calculated using SOC concentration ( $g\ C/kg$   
475 soil), bulk density (BD,  $kg/m^3$ ) and soil depth (m).

$$476 \text{SOC}_{stock} = \text{SOC}_{concentration} \times BD \times depth/100 \quad (2)$$

477  
478  
479 In the cases of MIMICS-PFT and MIMICS-ENV, the initial step involved grouping all pixels  
480 into four distinct plant functional groups or six environmental clusters. Since cross-validation  
481 was performed, the machine learning and process-based models were evaluated using test data,  
482 and the models with the optimal performance were subsequently employed at each pixel to  
483 estimate terrestrial SOC stocks. The map of ensemble estimate of SOC stocks was produced as  
484 the average of four model estimates at each pixel.

## 486 3. Results

### 487 3.1. Relative importance of environmental predictors of SOC concentration

488 Using the PVI in random forest, we identified the significance of environmental factors in  
489 predicting SOC concentration. At the continental scale, soil bulk density contributes most to the  
490 prediction of SOC concentration, following by MAT, NPP and MAP (Figure 3). Soil clay  
491 content and plant functional type exhibit relatively lesser significance in this regard.

492  
493  
494  
495 The relative predictor importance for forests and grasslands aligns with the importance at  
496 continental scale. In shrubland and woodland, NPP and MAP emerge as the pivotal factors.  
497 Collectively, across both continental and regional scales, soil bulk density, MAT, and MAP are  
498 the three most influential abiotic factors.

Deleted: To

Deleted: examine

Deleted: , we generated pixel-based SOC maps utilizing the four models validated within this study

Formatted: Superscript

Formatted: Superscript

Formatted: Centred

Deleted: .

Deleted: segregating

Deleted: also

Deleted: s

Deleted: Dominant

Deleted: controls

Deleted: Permutation Variable Importance (Permutation Variable Importance (

Deleted: ))

Deleted: is the most influential driver of SOC concentration variations

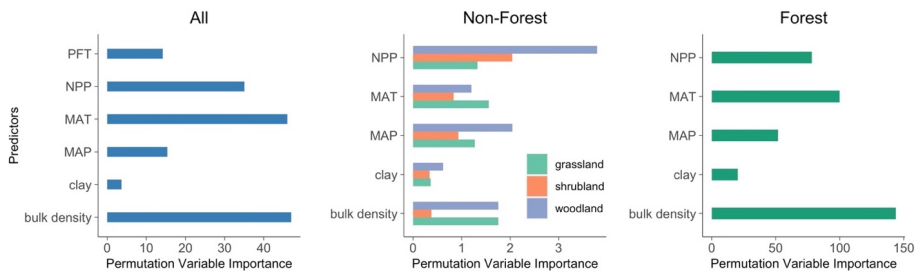


**Figure 3.** Importance of predictors on SOC concentration for different plant functional types.

### 3.2. Data clustering based on environmental factors

To develop the calibration groups for MIMICS-ENV, we partitioned the top three important abiotic factors, which are soil bulk density, MAT and MAP, into six distinct clusters using K-means (see Section 2.3). The resulting characteristics and spatial distribution of SOC belonging to these six clusters are illustrated in Figure 4.

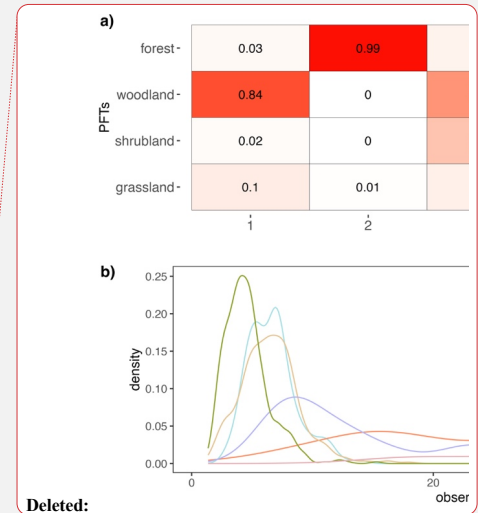
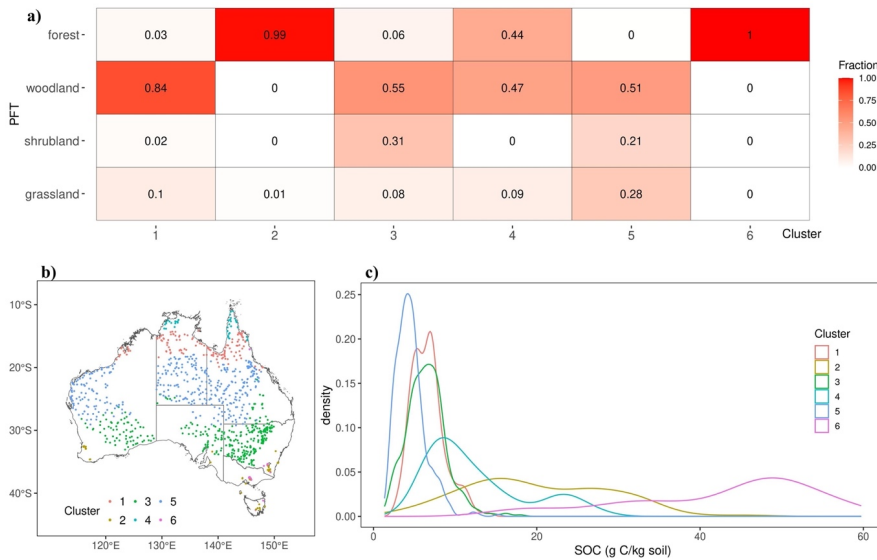
Notably, a substantial majority of forests were assigned to clusters 2 and 6 (Figure 4a), while woodland, shrubland, and grassland observations were distributed across the remaining four clusters. Among these clusters, cluster 5 exhibits the lowest SOC concentration, while SOC of cluster 1 and 3 display a comparable pattern but spread across different biomes. Conversely, distribution of SOC concentration in clusters 2, 4, and 6 shows more pronounced variability (Figure 4c).

Deleted: SOC

Deleted: s

Deleted: for

Deleted: 4b



Deleted:

534 **Figure 4. a)** Fraction of different PFT in each cluster divided based on environmental factors, **b)** spatial  
 535 **distribution of SOC observations from different environmental clusters** and **c)** density plot of observed SOC  
 536 **concentration for different clusters.**

Deleted: s

Deleted: (a)

Deleted: (b)

538

### 539 3.3. Evaluation of model performance

540

541 All models employed in this study (RF, K-means + MLR, MIMICS-PFT and MIMICS-ENV)  
 542 predicted SOC concentration well for both training data and test data (Figure 5). As anticipated,  
 543 sample data versus in-sample training or calibration data. When using test data, the mean value  
 544 of  $R^2$  for all models ranges from 0.82 to 0.94, mean LCCC ranges from 0.90 to 0.97, mean  
 545 RMSE ranges from 2.88 to 4.51 g C/kg soil, and mean MAE ranges from 1.55 to 2.57 g C/kg  
 546 soil.

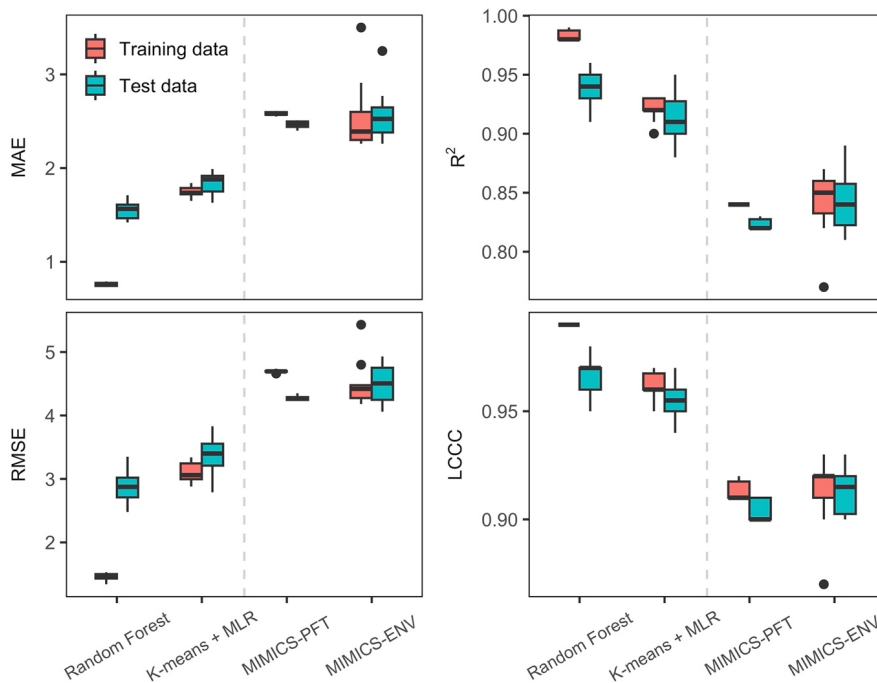
Deleted: performance for both process-based model and machine learning models degrade using out-of-

547

548 The machine learning models outperformed MIMICS in predicting SOC concentration,  
 549 regardless of the optimisation approach taken. Particularly, the **RF model** demonstrated the most  
 550 accurate predictions characterized by higher  $R^2$  and LCCC values and lower RMSE and MAE  
 551 values for both training and test data. While MIMICS-ENV displayed performance similar to  
 552 that of MIMICS-PFT in SOC concentration predictions based on RMSE and MAE, the former  
 553 exhibited slightly superior median  $R^2$  and LCCC values **but with a higher variability** (Figure 5).

Deleted: random forest

Deleted: algorithm

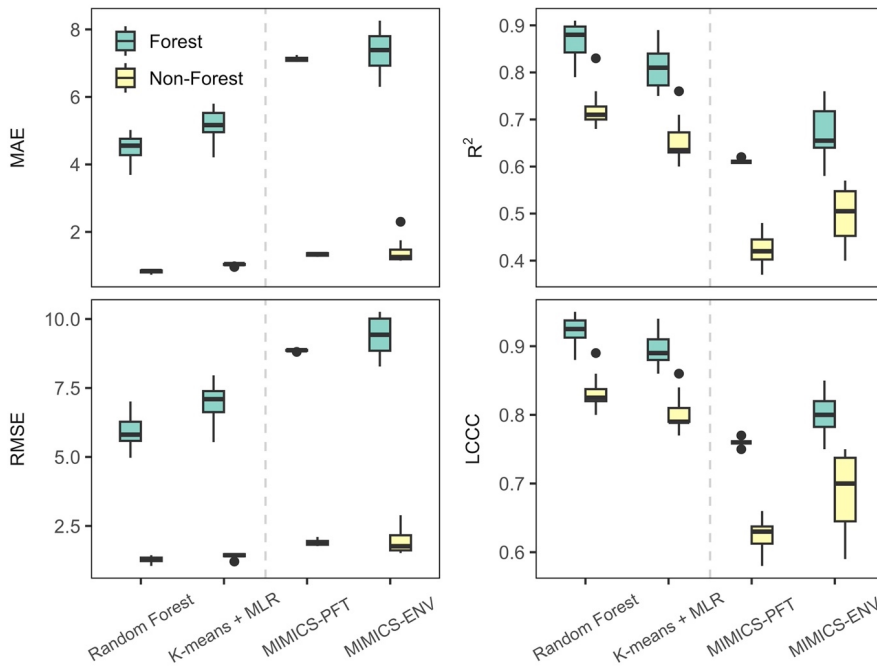


562  
 563 **Figure 5.** Performance metrics of SOC concentration predictions. Units for MAE and RMSE are g C/kg soil.  
 564 Centre line represents median value, and upper and lower box boundaries represent third and first quartile of  
 565 metrics from cross-validation. Whiskers extend to the smallest and largest values within 1.5 times the  
 566 interquartile range.

567  
 568 SOC concentration in forest soil exhibited significantly higher predictability than those in non-  
 569 forest (woodland, shrubland and grassland) soil, evidenced by higher  $R^2$  (ranging from 0.58 to  
 570 0.91) and LCCC (ranging from 0.75 to 0.95) for test data (Figure 6). Machine learning models  
 571 surpassed MIMICS in predicting SOC concentration for both forest and non-forest soils.  
 572 Notably, MIMICS-ENV outperformed MIMICS-PFT in SOC concentration predictions,  
 573 particularly in non-forest soils.

574  
 575

Deleted: algorithms



577  
 578  
 579 **Figure 6.** Performance metrics of SOC concentration predictions for forest and non-forest (woodland,  
 580 shrubland and grassland) soils in test (out-of-sample) data. Unit for MAE and RMSE is g C/kg soil. Centre  
 581 line represents median value, and upper and lower box boundaries represent third and first quartile [of metrics](#)  
 582 [from cross-validation](#). Whiskers extend to the smallest and largest values within 1.5 times the interquartile  
 583 range.

584  
 585 **3.4. Estimations of terrestrial SOC stocks**  
 586  
 587 [Using the best fitted models after cross-validation \(see Section 2.6 for details\), we estimated](#)  
 588 [the total amount of SOC stocks in the top 30 cm for the whole Australia continent at a spatial](#)  
 589 [resolution of 0.05° by 0.05°](#). The optimized parameters used for MIMICS-PFT and MIMICS-  
 590 [ENV at continental scale are shown in Table 3.](#)

591  
 592  
 593  
 594  
 595  
 596  
 597  
 598  
 599

Table 3. Optimized parameter ranges of MIMICS for cross-validation. Values in brackets were used for estimating SOC stocks at continental scale. See Table 1 for further explanations of each parameter.

Model	PFT/Cluster	$a_v$	$a_k$	$x_{desorp}$	$x_{beta}$	$x_{diffsoc}$
MIMICS-PFT	Grassland	4.36-18.11 (5.45)	4.42-19.11 (5.62)	1.90-3.0 (2.97)	1.06-1.42 (1.06)	16.21-29.90 (29.3)
	Shrubland	12.15-17.91 (12.46)	14.46-18.87 (16.80)	1.54-2.92 (2.58)	1.14-1.27 (1.24)	20.21-29.96 (29.73)
	Woodland	8.41-17.01 (10.92)	9.35-16.99 (12.73)	1.12-1.23 (1.10)	1.12-1.23 (1.18)	20.17-29.96 (23.91)
	Forest	3.15-8.56 (4.70)	12.61-19.69 (13.53)	0.39-3.0 (1.36)	1.42-1.88 (1.35)	11.55-27.70 (10.20)
	Cluster 1	5.23-13.82 (10.189)	6.08-17.80 (11.93)	1.62-2.85 (1.84)	1.07-1.20 (1.07)	0.00-29.81 (28.80)
MIMICS-ENV	Cluster 2	3.56-10.76 (7.60)	7.36-18.24 (15.70)	1.01-2.94 (2.07)	1.05-1.07 (1.05)	3.61-12.75 (6.91)
	Cluster 3	8.31-10.52 (8.48)	15.98-19.91 (19.66)	1.84-2.83 (2.25)	1.36-1.52 (1.52)	10.83-29.45 (26.25)
	Cluster 4	2.47-5.52 (5.10)	6.44-16.80 (13.52)	0.54-1.78 (0.92)	1.21-1.74 (1.42)	14.75-28.91 (20.37)
	Cluster 5	12.24-20.57 (19.55)	10.90-17.56 (17.56)	2.89-3.0 (2.98)	1.05-1.06 (1.05)	25.32-29.83 (25.75)
	Cluster 6	3.25-7.18 (6.40)	7.73-18.23 (15.86)	1.91-2.97 (2.73)	1.05-1.09 (1.09)	6.19-28.57 (15.47)

Formatted Table

Descriptive statistics of predicted terrestrial SOC stocks at 0-30 cm soil depth are shown in Table 4. Forests have the largest mean SOC stocks ranging from 70.3 to 113.9 t ha<sup>-1</sup> by all models, and shrubland is estimated to have the lowest mean SOC stocks. The distributions of predicted continental SOC stocks by all models are positively skewed with most estimated SOC stocks less than 50 t ha<sup>-1</sup> (Figure 7a), and SOC stocks at peak density predicted by MIMICS-ENV and MIMICS-PFT are smaller than those predicted by the two machine learning approaches.

Deleted: 3

Deleted: t/ha

Deleted: t/ha

Deleted: The maximum value of SOC stocks predicted by all models vary considerably.

Deleted: greater

Deleted: Notably, MIMICS-ENV depicted a pronounced deficit of SOC in central Australia, a distinctive pattern compared to the predictions of other models.

As expected, all models consistently projected larger SOC stocks in the southeast region, southwest corner and Tasmania, and consistently indicated lower SOC stocks in central and western Australia (Figure 7b). Among the models, K-means coupled with multiple linear regression consistently provided the highest SOC estimations across all vegetation types, while MIMICS-PFT model consistently yielded the lowest mean SOC stocks.

Deleted: approach

Deleted: The

Deleted: 9.3

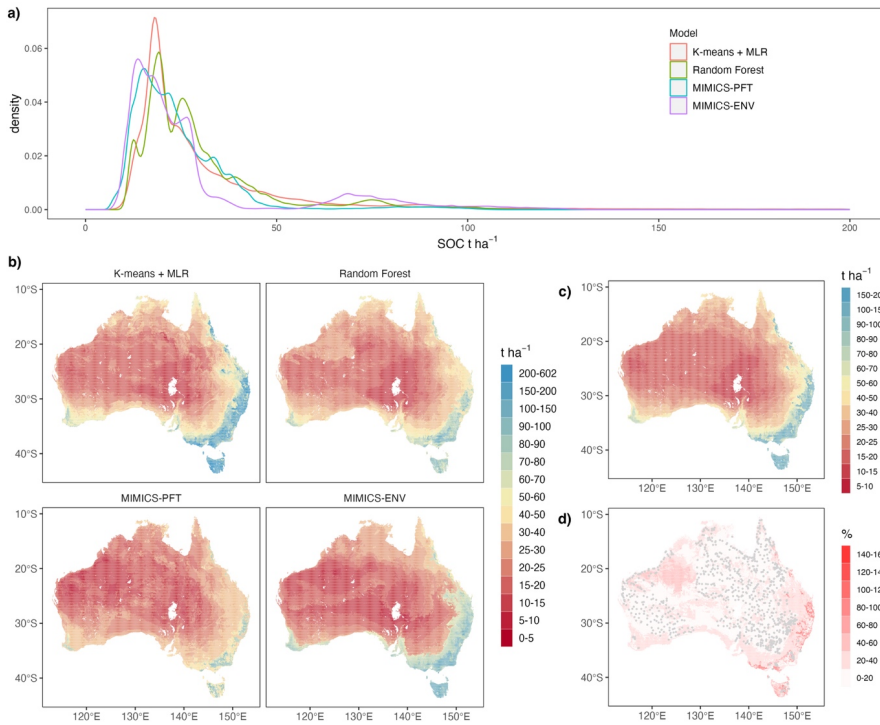
Deleted: t/ha

Deleted: 1

Deleted: t/ha

Deleted: The standard deviation

The ensemble estimate of SOC stocks (Figure 7c) shows a similar distribution pattern as that generated by single model. SOC stocks of the ensemble range from 10.0 to 180.4 t ha<sup>-1</sup> with an average value of 30.3 t ha<sup>-1</sup>. Coefficient of variation calculated as the ratio of standard deviation to mean across the four estimates (Figure 7d) is positively correlated with the ensemble mean estimate. That is, soils with higher SOC stocks exhibit greater variability in SOC predictions among different models. Note also that the variability of estimates tends to be smaller in areas with denser numbers of observations (Figure 7d).



641

642

643

644

645

646

647

648

649

650

651

**Figure 7.** Estimated Australian terrestrial SOC stocks ( $t\ ha^{-1}$ ) for top 30 cm soil and ensemble statistical characteristics: a) density plot of estimated terrestrial SOC stocks by all models, noting that only stocks less than  $200\ t\ ha^{-1}$  are shown for better comparison of the distribution; b) estimated SOC stocks by each model; c) estimated SOC stocks of the ensemble; d) coefficient of variation of the ensemble estimates of SOC stocks. Grey points represent locations of SOC observations.

**Table 4.** Descriptive statistics of estimated terrestrial SOC stocks ( $t\ ha^{-1}$ ) at 0-30 cm soil. Min. and Max. are minimum and maximum value, respectively. 1<sup>st</sup> Qu and 3<sup>rd</sup> Qu are first and third quartile, respectively.

	PFT	Min.	1 <sup>st</sup> Qu	median	mean	3 <sup>rd</sup> Qu	Max.
K-means + MLR	grassland	4.2	17.9	21.2	41.5	42.5	601.1
	shrubland	7.2	16.4	19.3	23.6	24.4	472.2
	woodland	7.1	20.1	26.1	33.3	33.7	483.1
	forest	18.0	51.3	95.2	113.9	153.4	474.0
	all	4.2	18.1	23.6	38.2	36.7	601.1
Random Forest	grassland	10.4	18.5	26.0	30.4	37.2	125.3
	shrubland	10.3	17.0	19.6	21.4	24.4	104.4
	woodland	10.5	20.3	25.8	28.2	32.4	122.1
	forest	29.3	55.0	82.3	78.4	97.0	161.7
	all	10.3	18.9	25.0	29.8	33.7	161.7
	grassland	10.8	16.4	24.1	25.1	33.3	58.7

Deleted:

Deleted: Predicted

Deleted: t/ha

Formatted: Line spacing: Multiple 1.2 li

Deleted: t/ha

Deleted: Predicted

Deleted: for

Deleted: Predicted

Deleted: standard

Deleted: deviation stocks within

Deleted: ¶

Deleted: 3

Deleted: predicted

Deleted: t/ha

Formatted: Font: 10.5 pt

Deleted: 1



MIMICS-PFT	shrubland	6.5	12.2	15.5	16.5	20.6	56.5
	woodland	7.8	17.4	21.2	22.1	25.9	61.4
	forest	17.9	44.5	77.4	70.3	88.5	109.9
	all	6.5	15.7	21.2	24.3	28.9	109.9
MIMICS-ENV	grassland	6.8	13.7	18.7	29.9	27.6	124.0
	shrubland	6.7	13.4	16.7	18.3	20.2	131.9
	woodland	8.1	18.0	24.0	27.5	28.0	131.6
	forest	15.8	35.7	90.4	79.4	106.5	134.1
	all	6.7	15.0	20.2	28.9	27.5	134.1
	grassland	11.4	17.1	21.1	31.7	36.3	180.4
	shrubland	10.0	15.2	17.3	20.0	21.7	170.4
Ensemble	woodland	11.0	18.8	24.4	27.8	30.0	168.0
	forest	22.0	46.8	93.1	85.5	112.7	166.3
	all	10.0	17.2	22.2	30.3	31.5	180.4

671

## 672 4. Discussion

### 673 4.1. Relative importance of predictors on SOC variations

674

675

676

677

678

679

680

681

682

683

684

685

686

687

688

689

690

691

692

693

694

695

696

697

698

699

700

701

Extensive research has been conducted to discern the factors that govern SOC concentration/stocks. Among the commonly employed predictors for SOC spatial variations, climate, organisms, topography, parent material, and soil properties are prominent (Wiesmeier et al., 2019). Within this study, we conducted a comparative assessment of the significance of key variables, namely MAT, MAP, NPP, soil clay content and bulk density, in driving variations in SOC in Australia. Although the number of predictors utilized in our approach is fewer than that employed in most digital mapping methodologies, our models show good performance in predicting SOC in Australia (Figure 5 and 6) and its strength lies in the potential for a more direct comparison between empirical and process-based models.

Consistent with the result by Hobley et al., (2015) on the soils from eastern Australia, this study identified soil bulk density as an important predictor of SOC concentration at continental scale (Figure 3). However, the relationship is largely interactive between soil bulk density and soil carbon concentration, (Murphy, 2015). Higher concentrations of soil organic matter facilitate soil aggregation formation and increase soil porosity, which results in lower bulk density. Meanwhile, a soil with reduced bulk density exhibits higher permeability for water and oxygen, which enhances plant root growth and SOC dynamics. Physically, the bulk density of organic matter is less than  $1 \text{ g cm}^{-3}$ , much lower than soil mineral solids with a density of  $2.66 \text{ g cm}^{-3}$ , therefore lower bulk density soils usually have higher SOC concentration (Marshall and Holmes, 1988).

Across the Australia continent, MAT emerges as the second most influential factor governing SOC variations, followed by NPP, MAP, and clay content. This sequence of significance diverges from the findings of Walden et al. (2023), where the order of importance was observed as  $\text{NPP} > \text{clay content} > \text{MAP} > \text{MAT}$  on a continental scale in Australia. The number of predictors used in their study is much higher than that in our study, which may affect the contribution of given predictors in SOC variation (Guo et al., 2019). This discrepancy might

Deleted: 4.2

Deleted: 7.9

Deleted: 5.4

Deleted: 6.9

Deleted: 3

Deleted: 4.4

Deleted: 9.9

Deleted: 3.4

Deleted: 6

Deleted: 5.3

Deleted: 4.9

Deleted: 4.7

Deleted: 6.3

Deleted: 8.4

Deleted: 31.3

Deleted: 9.6

Deleted: 53.1

Deleted: 2

Deleted: 81.6

Deleted: 4.2

Deleted: 10.5

Deleted: 1.9

Deleted: 1

Deleted: 33.2

Deleted: content

Deleted: While

Deleted: S

Deleted: is the most

Deleted: driver

Deleted: the

Deleted: The role of soil bulk density in SOC has been noted before in eastern Australia (Hobley et al., 2015). Soil bulk density is mainly a function of the parent material, soil genesis as well as soil aggregate formation

Deleted: Don et al., 2007

Deleted:

Deleted: A

Deleted: superior structural organization

Formatted: Superscript

Formatted: Superscript

Deleted: and an expanded surface area, facilitating enhanced retention of organic carbon (Lobsey and Viscarra Rosset, 2016). Subsequently, with

Deleted: a slightly lower value of importance than soil bulk density

Deleted: more

746 however be attributable to the utilization of observations encompassing both terrestrial and blue  
747 carbon ecosystems in their study. Clay emerges as key driver mainly in the groups where aquatic  
748 plants (e.g., seagrass, tidal marsh) appeared. The more extensive dataset encompassing the  
749 eastern coastline, characterized by greater variability and abundance of NPP input, potentially  
750 elevates NPP to a dominant role in influencing SOC variations within their study.

751  
752 For SOC in different vegetation types (Figure 3), soil bulk density and MAT are more important  
753 than other factors in forest, and all factors except clay content showed similar importance in  
754 predicting SOC concentration in grassland. NPP and MAP dominate the SOC variations in  
755 woodland and shrubland. Climate conditions as represented by MAT and MAP exert their  
756 impact on SOC in all vegetation types. It was proposed that the primary climatic determinant  
757 of SOC variation hinges on the primary constraint affecting SOC production and turnover  
758 (Hobley et al., 2016). In this study, most shrublands and woodlands are distributed in arid and  
759 semi-arid regions characterized by limited precipitation, which leads to water stress in surface  
760 soil, limiting plant productivity and reducing soil C input (Hobley et al., 2015). Consequently,  
761 MAP and NPP exhibited relatively higher influence on SOC variations in soils under these  
762 vegetation types. In contrast, forest SOC observations are mainly distributed in areas with  
763 relatively lower temperatures, therefore experience constrained microbial metabolism, leading  
764 to reduced decomposition rates and the high accumulation of SOC (Wynn et al., 2006).  
765 Consequently, MAT emerges as a key factor influencing SOC variations in forests. Furthermore,  
766 it is noteworthy that soil bulk density plays a crucial role in determining SOC distribution within  
767 forest, where it is found to be significantly lower compared to other vegetation types. This lower  
768 soil bulk density likely improves oxygen availability to soil microbial communities, and  
769 facilitates the formation of microaggregates to enhance the preservation of SOC within the soil  
770 matrix (Bronick and Lal, 2005). Consequently, it effectively contributes to elevated SOC  
771 concentration levels in forested areas.

772  
773 PFT is the only categorical predictor for SOC concentration in this study. SOC is mainly derived  
774 from plant C input through above-/belowground tissues, and SOC turnover and storage are  
775 influenced by plant traits like plant growth rate and chemical and physical composition (De  
776 Deyn et al., 2008; Faucon et al., 2017). With shared representation of similar plant traits, PFT  
777 is widely used in process-based models (Poulter et al., 2015; Famiglietti et al., 2023). It was  
778 found that the vertical distribution of SOC is highly related to PFT due to the different root  
779 distribution and above- and belowground allocation (Jobbágy and Jackson, 2000). However,  
780 our study is limited by the absence of SOC observations at multiple soil depths, restricting the  
781 analysis to the spatial distribution of SOC at 30 cm soil depth. The influence of PFT on SOC  
782 concentration at this particular depth appears relatively insignificant (Figure 3), casting doubt  
783 on the effectiveness of optimizing parameters of process-based models s for individual PFT  
784 (Cranko Page et al., 2023). Considering this, employing the top 3 influential abiotic predictors,  
785 soil bulk density, MAT, and MAP, we partitioned all observations into six distinct clusters using  
786 K-means. It was anticipated that SOC ranges within each cluster would be narrow due to the  
787 high similarity of these three predictors within each group. However, the distribution of SOC

Deleted: driving

Deleted: ecosystems

Deleted: and

Deleted: s

Deleted: s

Deleted: are

Formatted: Line spacing: Multiple 1.2 li

Deleted: s

Deleted: are

Deleted: s

Deleted: s

Deleted: s

799 in clusters 2, 4, and 6 exhibited considerable variability (Figure 4). Given that these clusters are  
800 predominantly composed of forests, it becomes apparent that these three abiotic factors alone  
801 are insufficient to fully characterize the intricacies of forest SOC concentration. It was found  
802 that elevation and evapotranspiration also drive the variation of forest SOC in Australia (Walden  
803 et al., 2023), and taking them into account might potentially increase the predictability of forest  
804 SOC.

Deleted:

Deleted: ecosystems

Deleted: ¶

#### 805 4.2. Model evaluation and comparison with other studies

806 Although the predictors used for machine learning models are not exactly same as the inputs of  
807 MIMICS, the missing factors (e.g., MAP) were used for parameter optimization of MIMICS-  
808 ENV, making the predictions dependent on similar information and so comparable to some  
809 extent. Besides, our study presented clear evaluation metrics for out-of-sample validation,  
810 enabling a more robust assessment of model performance when applied to new datasets.

812 Based on the performance metrics of test data, the machine learning models performed  
813 remarkably well (Figure 5). The  $R^2$  suggested that both machine learning models can explain  
814 more than 90% of SOC variability across sites, and random forest did the best job with greatest  
815  $R^2$  and LCCC, and lowest MAE and RMSE. Random forest algorithms were widely adopted in  
816 predicting spatial-temporal SOC dynamics and produced moderately good performance  
817 regionally and globally. For example, Wang et al. (2022) applied random forest to estimate SOC  
818 stocks in south-eastern Australia and explained 69% of the variation of current SOC stocks.  
819 Nyaupane et al. (2023) trained a random forest model using global SOC observations and  
820 explained 61% of SOC variation. The good performance of random forest might be attributed  
821 to reduced susceptibility to over-fitting and better capacity to manage the hierarchical non-  
822 linear relationships that exist between SOC and environmental predictors (Wang et al., 2018b).  
823 Other machine learning methods have been applied to predict continental SOC stocks in  
824 Australia. For example, Walden et al. (2023) trained regression-tree algorithm CUBIST to  
825 predict SOC stocks for top 30 cm soil using the harmonised datasets. The mean LCCC and  
826 RMSE for out-of-sample validation in their study was 0.78 and 0.20 respectively when  $\log_{10}$   
827 transformed SOC ( $t\ ha^{-1}$ ) values were used. Wadoux et al. (2023) applied quantile regression  
828 forest to predict SOC stocks at multiple soil depths. The prediction accuracy decreased  
829 dramatically for deeper depth intervals with the greatest  $R^2$  (0.53) at 0-5 cm soil. The better  
830 results in this study may be attributed to the removal of cropland ecosystems, which are clearly  
831 highly managed and so less predictable. Agricultural practices greatly affect SOC stocks in  
832 Australia and add the complexity to the relationship between SOC and environmental factors  
833 (Luo et al., 2010). Models using environmental predictors without representation of land use  
834 management are unlikely to be able to fully capture the SOC dynamics in croplands (Abramoff  
835 et al., 2022).

Deleted: two

Deleted: well

Deleted: at 30 cm soil

Deleted: t/ha

Deleted: content

837 Although MIMICS was not as accurate as machine learning models in simulating spatial  
838 variation of SOC concentration in Australia, it did well at continental scale with mean  $R^2$  at  
839 0.82 and 0.84 for MIMICS-PFT and MIMICS-ENV, respectively (Figure 5), much greater than  
840

Deleted: made less

Deleted: estimations of SOC than machine learning models

851 the values (<0.4) obtained by Abramoff et al. (2022) who applied a different microbial explicit  
852 model to Australian SOC dataset. Georgiou et al. (2021) found that there was a mismatch  
853 between observations and MIMICS in the role of different environmental controls on SOC  
854 variability at global scale. In their study, NPP and MAT had the most explanatory power for  
855 SOC stocks from MIMICS, while clay content had the most explanatory power for global SOC  
856 observations, which limits the predictability of SOC using MIMICS in their study. However, in  
857 our study, NPP and MAT rather than clay content played a greater role in observed SOC  
858 variations, perhaps contributing to a better performance of MIMICS in Australia. It also means  
859 that SOC estimates in our study are highly sensitive to the estimates of NPP. In this study, we  
860 used MODIS NPP product (Running and Zhao, 2021) and did not account for the loss of NPP  
861 due to human activities, which may likely influence the optimized estimates of some model  
862 parameters, and the uncertainties of simulated SOC concentration. Future studies would ideally  
863 use multiple NPP products to quantify the impacts of NPP uncertainties in simulating SOC  
864 variation in Australia.

866 The modest performance of process-based model MIMICS relative to machine learning models  
867 could potentially be attributed to the absence of explicit representation of MAP. The  
868 augmentation of MAP within parameter optimization in MIMICS-ENV did allow improved  
869 performance compared to MIMICS-PFT, particularly within non-forest regions where the  
870 importance of MAP rivals or surpasses that of temperature. Precipitation is a determinant of  
871 plant productivity, especially in arid and semi-arid regions. Besides, arid regions with limited  
872 precipitation are characterized by lower weathering rate limiting the formation of mineral-  
873 associated soil carbon (Doetterl et al., 2015). Hence, we assume that introducing the effect of  
874 moisture to MIMICS could contribute to more accurate prediction of SOC, as compared with  
875 just taking MAP into account for parametrization, especially in arid and semiarid regions.

877 All models produced lower MAE and RMSE for non-forest SOC but higher R<sup>2</sup> and LCCC for  
878 forest SOC (Figure 6). SOC in forest is more abundant and variable compared to SOC in other  
879 vegetation types even when climate conditions are similar, which leads to greater absolute error  
880 in the estimated forest SOC than in other vegetation types. However, in terms of the consistency  
881 and concordance between the pattern of observations and predictions, all models show higher  
882 ability to predict SOC in forest. Forests, given that they are less perturbed ecosystems, might  
883 show greater SOC predictability due to the reduced influence of direct anthropogenic  
884 disturbances. Grasslands, shrublands, and woodlands, predominantly situated in Australian  
885 rangelands may experience extensive grazing and land management. Primarily, grazing reduces  
886 soil carbon input by consumption of aboveground biomass and accelerate SOC decomposition  
887 through input of nutrient-enriched animal waste. This introduces additional uncertainties to our  
888 modelled SOC estimates, since C input is represented solely by NPP without accounting for the  
889 impact of grazing and land managements. Moreover, the cascading effects of grazing extend to  
890 potential alterations in plant composition and structural attributes, inducing consequential shifts  
891 in litter properties that modulate soil carbon decomposition kinetics (Lunt et al., 2007; Bai and  
892 Cotrufo, 2022). The disturbances triggered by grazing manifest in soil carbon pools, leading to

Deleted: in explaining

Deleted: constrains the accuracy of

Deleted:

Deleted: estimation

Deleted: the higher R<sup>2</sup> and LCCC mean that

Deleted: forest

Deleted: using environmental predictors.

Deleted: afford

Deleted: This stands in contrast to ecosystems like grasslands

Deleted: where

Deleted: constitutes the predominant agricultural practice.

Deleted: leads to a reduction in

Deleted: flux

Deleted: originating from

Deleted: .

Deleted: This intricate interplay of grazing-induced disturbances introduces a layer of complexity to SOC predictions. ...

911 a state of disequilibrium rather than adhering to the assumption of SOC convergence toward  
912 equilibrium, as embraced in this study's framework. Notably, forests, as relatively undisturbed  
913 natural ecosystems, demonstrate a better coherence with the equilibrium assumption, rendering  
914 their SOC more amenable to prediction through environmental drivers.

#### 915 916 4.3. Spatial prediction of SOC stocks in Australia

917  
918 We produced gridded SOC stocks across Australia using the models validated in this study and  
919 an ensemble estimate as the average of four models (Figure 7). Among the models, K-means  
920 coupled with multiple linear regression produced the largest mean SOC stocks both at  
921 continental scale and for all vegetation types. In contrast, RF and MIMICS with different  
922 parameterization approaches produced lower SOC stock estimations (Table 4). The mean  
923 terrestrial SOC stocks estimated by random forest and MIMICS are comparable with that  
924 estimated by Australian baseline map, which was generated using machine learning algorithm,  
925 reporting mean SOC stocks at  $29.7 \text{ t ha}^{-1}$ , with 95% confidence limits of 22.6 and  $37.9 \text{ t ha}^{-1}$   
926 (Viscarra Rossel et al., 2014). However, SOC stocks might be underestimated by these methods  
927 because of the scarcity of data from the most productive temperate forest both in the baseline  
928 map (Bennett et al., 2020) and in our study. Parameter optimization process of MIMICS and  
929 the training process of random forest are greatly affected by data used to train the model. Most  
930 SOC observations in this study were sourced from arid and semiarid regions, characterized by  
931 relatively low SOC content. As a result, the models' ability to predict SOC stocks beyond the  
932 observed data range is somewhat constrained. PFT was found to be less important than other  
933 environmental factors in driving spatial SOC variations (Figure 3), so it was perhaps not  
934 surprising that applying parameters optimized for each plant functional type to the regions with  
935 same PFT but broader climate conditions led to inferior results than applying parameters  
936 optimized for each environmental group.

937  
938 The utilization of linear regression in K-means + MLR generated SOC estimates beyond the  
939 range of observations, particularly in eastern Australia where environmental conditions deviate  
940 from the training data. The mean SOC stocks estimated by K-means + MLR ( $38.2 \text{ t ha}^{-1}$ ) are  
941 higher than those of the other models employed in this study, and align closely with the mean  
942 value  $36.2 \text{ t ha}^{-1}$ , reported by Walden et al. (2023) who updated the Australian baseline SOC  
943 map (Viscarra Rossel et al., 2014) by incorporating additional SOC observations from forests  
944 and coastal marine ecosystems. However, caution is required when interpreting extreme values  
945 derived from the K-means + MLR, such as the instance of grassland SOC stocks reaching  $601$   
946  $\text{t ha}^{-1}$  (Table 4). These values raise concerns about the reliability of this approach when  
947 extrapolating out-of-sample. Though there is a positive relationship between NPP and SOC  
948 observations in this study, SOC accumulation cannot continuously increase linearly in the  
949 regions where environmental conditions seem highly conducive to SOC formation. The greater  
950 amount of carbon input in eastern Australia might trigger the acceleration of microbial  
951 decomposition because of a priming effect, and lead to a decreased accumulation of SOC stocks  
952 (Ren et al., 2022). The existence of SOC saturation also implies that SOC cannot be

Deleted: random forest

Deleted: more conservative

Deleted: the

Deleted: t/ha

Deleted: t/ha

Deleted: limited

Deleted: s

Deleted: t/ha

Deleted: t/ha

Deleted: t/ha

Deleted: 3

964 accumulated without limit (Georgiou et al., 2022; Viscarra Rossel et al., 2023). In light of these  
965 complexities, applying linear regression to predict SOC stocks, especially under the extreme  
966 environmental conditions, should be undertaken with care.

Deleted: content

967  
968 Continentally, higher SOC stocks were estimated for the southwest corner and southeast  
969 Australia (Figure 7), aligning with other SOC maps for Australia (Wadoux et al., 2023; Walden  
970 et al., 2023). These regions are characterized by lower temperature and higher precipitation,  
971 therefore high SOC accumulation appeared because of high carbon input of NPP and low  
972 decomposition rate. However, the high variability of SOC estimates among the four models in  
973 these regions should be highlighted (Figure 7d), along with the difference of magnitudes  
974 between the estimates in this study and other Australian SOC products (Viscarra Rossel et al.,  
975 2014; Walden et al., 2023). Despite inherent differences in model structures, the scarcity of  
976 observations in these regions likely contributes to the large uncertainties in SOC estimates.

Deleted: as

Deleted: .

Deleted: stimulation of NPP by moisture and the constrained microbial metabolism in low temperatures.

977 Forest has the largest mean SOC stocks ranging from 70.3 to 113.9  $t\ ha^{-1}$ , estimated by four  
978 models in this study. Around 75% of the forest SOC is from soil under Eucalypt open forest,  
979 and mean SOC stocks under this type of forest were estimated to be 87.5  $t\ ha^{-1}$  (63.8 -119.6  $t$   
980  $ha^{-1}$  for 95% confidence interval) (Walden et al., 2023). Shrublands are estimated to have the  
981 lowest mean SOC stocks, and more than 90% of shrub SOC observations are from soil under  
982 Acacia shrubland and Chenopod shrubland, which rank at the bottom of SOC stocks among  
983 different vegetation types (Walden et al., 2023). The low SOC in shrubland is probably due to  
984 low carbon input because of limited rainfall (MAP < 280 mm). Though the mean SOC stocks  
985 in non-forest regions are much smaller than that for forest, the greater area of vegetation cover  
986 results in considerable total SOC stocks, highlighting the importance of carbon building and  
987 maintaining via improved managements in these areas. Greater variability of SOC estimates  
988 among different models appears in the regions where SOC stocks are higher (Figure 7). The  
989 sparsity of SOC observations is a primary contributor to the uncertainties associated with SOC  
990 estimates in these regions, highlighting the importance on continual collection of data to better  
991 constrain models' behaviour. This imperative is especially pronounced in regions covered by  
992 forests, as forested soils exhibit substantial SOC stocks, amplifying the significance of abundant  
993 and accurate data acquisition in these specific ecosystems.

Deleted: t/ha

Deleted: t/ha

Deleted: t/ha

## 994 5. Conclusion

995  
996 We compared the performance of two machine learning models, and one process-based  
997 microbial model employing two parameterization approaches, to explain the spatial variation  
998 of SOC concentration in the top 30 cm soil in Australia. We found that climate conditions and  
999 NPP contribute more than soil clay content in predicting SOC concentration in Australia.

Deleted: distinct

Deleted: explore

Deleted: the diversity of SOC estimates within a 30 cm soil depth...

Deleted: across

Deleted: Results

1000  
1001 Validation results affirm that with appropriate filtering of data (e.g. removing highly managed  
1002 crop ecosystems) models can predict SOC concentration at a continental scale with reasonably  
1003 high reliability, achieving explained variances exceeding 80% for out-of-sample test data, with  
1004 random forest showing highest prediction accuracy. Notably, all models show higher  $R^2$  in

Deleted: highlight soil bulk density and MAT as predominant factors governing SOC concentration variations, both on a continental scale and within forest and grassland ecosystems. Conversely, NPP and MAP exhibit greater significance in driving SOC variations within shrubland and woodland soil. Our study underscores the importance of including the influence of appropriate environmental factors in process-based models in different environments.

1027 prediction of SOC in forest than in non-forest soils. MIMICS, with parameters optimized for  
1028 different environmental clusters, performed better in SOC prediction than MIMICS with  
1029 parameters optimized for different PFT, especially in non-forest regions.

Deleted: under

Deleted: under

Deleted: vegetations

Deleted: s

1031 All models broadly agree on the spatial distribution of SOC stocks, with higher SOC stocks  
1032 concentrated in the southeast and southwest regions of Australia. However, the variations in  
1033 estimated values need to be acknowledged, particularly in highly productive regions. Among  
1034 these estimates, K-means algorithm coupled with multiple linear regression yields the highest  
1035 mean SOC stocks estimate, while the MIMICS-PFT model generates the lowest estimate.  
1036 Considerable disagreement of the maximum and minimum SOC stock values predicted by all  
1037 models exists partly because models are less constrained by observations in these environments,  
1038 highlighting the need for continued observational campaigns.

Deleted: most conservative

1039 Our investigation has revealed significant disparities in estimated SOC stocks when different  
1040 methodologies were employed. This highlights the need for a critical re-evaluation of land  
1041 management strategies that heavily depend on SOC estimates derived from a single approach.  
1042 The incorporation of an ensemble of SOC estimates is more likely to effectively capture  
1043 elements of the uncertainty associated with SOC estimations, providing a more robust basis for  
1044 informing strategies in soil carbon management and climate change mitigation.

## 1046 Code availability

1047 Source Code of vertically resolved MIMICS can be accessed at the CSIRO data portal  
1048 <https://doi.org/10.25919/843a-w584> (Wang et al., 2021). Codes for data analysis and machine  
1049 learning can be accessed by contacting the correspondence author.

## 1051 Data availability

1052 The SOC observations described in Viscarra Rossel et al. (2014), are not publicly available but  
1053 are available from Raphael A. Viscarra Rossel ([r.viscarra-rossel@curtin.edu.au](mailto:r.viscarra-rossel@curtin.edu.au)) on reasonable  
1054 request. All other data used in this study are publicly accessible and the specific references of  
1055 these databases are provided in Section 2.4.

Deleted: from VR dataset

Deleted:

## 1057 Author contribution

1058 Conceptualization: LW, GA, Y-PW, AP; Methodology: LW, GA, Y-PW; Investigation: LW,  
1059 RAVR; Formal analysis and Visualization: LW; Writing-original draft preparation: LW;  
1060 Writing-review & editing: LW, GA, Y-PW, AP, RAVR.

## 1062 Competing interests

1063 The co-author Raphael A. Viscarra Rossel is a member of the editorial board of SOIL.  
1064

1072 **Acknowledgements**

1073  
1074 LW thanks the China Scholarship Council and the University of New South Wales for financial  
1075 support during her PhD study. RAVR and Y-PW thank the Australian Research Council's  
1076 Discovery Projects scheme (project DP210100420) for funding. LW, GA and AP thank the ARC  
1077 Centre of Excellence for Climate Extremes for supporting this work (CE170100023).

1078  
1079  
1080

1081 **Reference**

1082  
1083 Abramoff, R. Z., Guenet, B., Zhang, H., Georgiou, K., Xu, X., Viscarra Rossel, R. A., Yuan, W.  
1084 and Ciais, P.: Improved global-scale predictions of soil carbon stocks with Millennial Version  
1085 2. *Soil Biol Biochem*, 164, 108466, <https://doi.org/10.1016/j.soilbio.2021.108466>, 2022.

1086 Abs, E. and Ferrière, R.: Modeling microbial dynamics and heterotrophic soil respiration: Effect  
1087 of climate change. *Biogeochemical cycles: ecological drivers and environmental impact*,  
1088 103-129, <https://doi.org/10.1002/9781119413332.ch5>, 2020.

1089 Adhikari, K., Mishra, U., Owens, P., Libohova, Z., Wills, S., Riley, W., Hoffman, F. and Smith,  
1090 D.: Importance and strength of environmental controllers of soil organic carbon changes with  
1091 scale. *Geoderma*, 375, 114472, <https://doi.org/10.1016/j.geoderma.2020.114472>, 2020.

1092 Bai, Y. and Cotrufo, M. F.: Grassland soil carbon sequestration: Current understanding,  
1093 challenges, and solutions. *Science*, 377, 603-608, doi: 10.1126/science.abo2380, 2022.

1094 Bennett, L. T., Hinko-Najera, N., Aponte, C., Nitschke, C. R., Fairman, T. A., Fedrigo, M. and  
1095 Kasel, S.: Refining benchmarks for soil organic carbon in Australia's temperate forests.  
1096 *Geoderma*, 368, 114246, <https://doi.org/10.1016/j.geoderma.2020.114246>, 2020.

1097 Bissett, A., Fitzgerald, A., Meintjes, T., Mele, P. M., et al.: Introducing BASE: the biomes of  
1098 Australian soil environments soil microbial diversity database. *GigaScience*, 5, s13742–  
1099 016–0126–5. <https://doi.org/10.1186/s13742-016-0126-5>, 2016.

1100 Bossio, D., Cook-Patton, S., Ellis, P., Fargione, J., Sanderman, J., Smith, P., Wood, S., Zomer,  
1101 R., Von Unger, M. and Emmer, I.: The role of soil carbon in natural climate solutions. *Nat*  
1102 *Sustain*, 3, 391-398, <https://doi.org/10.1038/s41893-020-0491-z>, 2020.

1103 Breiman, L.: Random forests. *Machine learning*, 45, 5-32,  
1104 <https://doi.org/10.1023/A:1010933404324>, 2001.

1105 Bronick, C. J. and Lal, R.: Soil structure and management: a review. *Geoderma*, 124, 3-22,  
1106 <https://doi.org/10.1016/j.geoderma.2004.03.005>, 2005.

1107 Cranko Page, J., Abramowitz, G., De Kauwe, M. G. and Pitman, A. J.: Are plant functional  
1108 types fit for purpose? *Geophys Res Lett*, 51, [e2023GL104962](https://doi.org/10.1029/2023GL104962),  
1109 <https://doi.org/10.1029/2023GL104962>, 2024.

1110 Chandel, A. K., Jiang, L. and Luo, Y.: Microbial Models for Simulating Soil Carbon Dynamics:  
1111 A Review. *J Geophys Res-Bioge*, e2023JG007436, <https://doi.org/10.1029/2023JG007436>,  
1112 2023.

Formatted: Font: (Default) Times New Roman, 12 pt, No underline, Font colour: Auto, Border: (No border), Pattern: Clear

Field Code Changed

Deleted: 2023 (accepted).



1114 De Deyn, G. B., Cornelissen, J. H. and Bardgett, R. D.: Plant functional traits and soil carbon  
 1115 sequestration in contrasting biomes. *Ecol Lett*, 11, 516-531, [https://doi.org/10.1111/j.1461-](https://doi.org/10.1111/j.1461-0248.2008.01164.x)  
 1116 [0248.2008.01164.x](https://doi.org/10.1111/j.1461-0248.2008.01164.x), 2008.

1117 Debeer, D. and Strobl, C.: Conditional permutation importance revisited. *BMC bioinformatics*,  
 1118 21, 1-30, <https://doi.org/10.1186/s12859-020-03622-2>, 2020.

1119 Doetterl, S., Stevens, A., Six, J., Merckx, R., Van Oost, K., Casanova Pinto, M., Casanova-  
 1120 Katny, A., Muñoz, C., Boudin, M. and Zagal Venegas, E.: Soil carbon storage controlled by  
 1121 interactions between geochemistry and climate. *Nat Geosci*, 8, 780-783,  
 1122 <https://doi.org/10.1038/ngeo2516>, 2015.

1123 Duan, Q., Gupta, V. K. and Sorooshian, S.: Shuffled complex evolution approach for effective  
 1124 and efficient global minimization. *J Optim Theory Appl*, 76: 501-521,  
 1125 <https://doi.org/10.1007/BF00939380>, 1993.

1126 Famiglietti, C. A., Worden, M., Quetin, G. R., Smallman, T. L., Dayal, U., Bloom, A. A.,  
 1127 Williams, M. and Konings, A. G.: Global net biome CO<sub>2</sub> exchange predicted comparably  
 1128 well using parameter–environment relationships and plant functional types. *Glob Change*  
 1129 *Biol*, 29, 2256-2273, <https://doi.org/10.1111/gcb.16574>, 2023.

1130 Faucon, M.-P., Houben, D. and Lambers, H.: Plant functional traits: soil and ecosystem services.  
 1131 *Trends Plant Sci*, 22, 385-394, <https://doi.org/10.1016/j.tplants.2017.01.005>, 2017.

1132 Georgiou, K., Malhotra, A., Wieder, W. R., Ennis, J. H., Hartman, M. D., Sulman, B. N., Berhe,  
 1133 A. A., Grandy, A. S., Kyker-Snowman, E. and Lajtha, K.: Divergent controls of soil organic  
 1134 carbon between observations and process-based models. *Biogeochemistry*, 156, 5-17,  
 1135 <https://doi.org/10.1007/s10533-021-00819-2>, 2021.

1136 Georgiou, K., Jackson, R. B., Vindušková, O., Abramoff, R. Z., Ahlström, A., Feng, W., Harden,  
 1137 J. W., Pellegrini, A. F., Polley, H. W. and Soong, J. L.: Global stocks and capacity of mineral-  
 1138 associated soil organic carbon. *Nat Commun*, 13, 3797, [https://doi.org/10.1038/s41467-022-](https://doi.org/10.1038/s41467-022-31540-9)  
 1139 [31540-9](https://doi.org/10.1038/s41467-022-31540-9), 2022.


1140 Grace, P. R., Post, W. M. and Hennessy, K.: The potential impact of climate change on  
 1141 Australia's soil organic carbon resources. *Carbon Balance Manag*, 1, 1-10,  
 1142 <https://doi.org/10.1186/1750-0680-1-14>, 2006.

1143 Grundy, M., Viscarra Rossel, R. A., Searle, R., Wilson, P., Chen, C. and Gregory, L.: Soil and  
 1144 landscape grid of Australia. *Soil Res*, 53, 835-844, <https://doi.org/10.1071/SR15191>, 2015.

1145 Guo, Z., Adhikari, K., Chellasamy, M., Greve, M. B., Owens, P. R. and Greve, M. H.: Selection  
 1146 of terrain attributes and its scale dependency on soil organic carbon prediction. *Geoderma*,  
 1147 340, 303-312, <https://doi.org/10.1016/j.geoderma.2019.01.023>, 2019.

1148 Heung, B., Ho, H. C., Zhang, J., Knudby, A., Bulmer, C. E. and Schmidt, M. G.: An overview  
 1149 and comparison of machine-learning techniques for classification purposes in digital soil  
 1150 mapping. *Geoderma*, 265, 62-77, <https://doi.org/10.1016/j.geoderma.2015.11.014>, 2016.

1151 Hobley, E., Wilson, B., Wilkie, A., Gray, J. and Koen, T.: Drivers of soil organic carbon storage  
 1152 and vertical distribution in Eastern Australia. *Plant Soil*, 390, 111-127,  
 1153 <https://doi.org/10.1007/s11104-015-2380-1>, 2015.

**Deleted:** Don, A., Schumacher, J., Scherer-Lorenzen, M., Scholten, T. and Schulze, E.-D.: Spatial and vertical variation of soil carbon at two grassland sites—implications for measuring soil carbon stocks. *Geoderma*, 141, 272-282, <https://doi.org/10.1016/j.geoderma.2007.06.003>, 2007. 

- 1159 Hobley, E. U., Baldock, J. and Wilson, B.: Environmental and human influences on organic  
 1160 carbon fractions down the soil profile. *Agric Ecosyst Environ*, 223, 152-166,  
 1161 <https://doi.org/10.1016/j.agee.2016.03.004>, 2016.
- 1162 [Jackson, R. B., Lajtha, K., Crow, S. E., Hugelius, G., Kramer, M. G. and Piñeiro, G.: The](#)  
 1163 [ecology of soil carbon: pools, vulnerabilities, and biotic and abiotic controls. \*Annual review\*](#)  
 1164 [of ecology, evolution, and systematics](#), 48, 419-445, [https://doi.org/10.1146/annurev-](https://doi.org/10.1146/annurev-ecolsys-112414-054234)  
 1165 [ecolsys-112414-054234](#), 2017.
- 1166 Jeffrey, S. J., Carter, J. O., Moodie, K. B. and Beswick, A. R.: Using spatial interpolation to  
 1167 construct a comprehensive archive of Australian climate data. *Environ Model Softw*, 16, 309-  
 1168 330, [https://doi.org/10.1016/S1364-8152\(01\)00008-1](https://doi.org/10.1016/S1364-8152(01)00008-1), 2001.
- 1169 Jenny, H.: Factors of soil formation: a system of quantitative pedology, [Agron. J.](#), 33, 857-858,  
 1170 <https://doi.org/10.2134/agronj1941.00021962003300090016x>, 1941.
- 1171 Jobbágy, E. G. and Jackson, R. B.: The Vertical Distribution of Soil Organic Carbon and Its  
 1172 Relation to Climate and Vegetation. *Ecol Appl*, 10, 423-436, [https://doi.org/10.1890/1051-](https://doi.org/10.1890/1051-0761(2000)010[0423:TVDOSO]2.0.CO;2)  
 1173 [0761\(2000\)010\[0423:TVDOSO\]2.0.CO;2](#), 2000.
- 1174 Keskin, H., Grunwald, S. and Harris, W. G.: Digital mapping of soil carbon fractions with  
 1175 machine learning. *Geoderma*, 339, 40-58, <https://doi.org/10.1016/j.geoderma.2018.12.037>,  
 1176 2019.
- 1177 Lamichhane, S., Kumar, L. and Wilson, B.: Digital soil mapping algorithms and covariates for  
 1178 soil organic carbon mapping and their implications: A review. *Geoderma*, 352, 395-413,  
 1179 <https://doi.org/10.1016/j.geoderma.2019.05.031>, 2019.
- 1180 Lawrence, I. and Lin, K.: A concordance correlation coefficient to evaluate reproducibility.  
 1181 *Biometrics*, 45, 255-268, <https://doi.org/10.2307/2532051>, 1989.
- 1182 [Le Noë, J., Manzoni, S., Abramoff, R., Bolscher T., Bruni, E., Cardinael, R., Ciais, P., Chenu,](#)  
 1183 [C., Clivot, H., Derrien, D., Ferchaud, F., Garnier, P., Goll, D., Lashermes, G., Martin, M.,](#)  
 1184 [Rasse, D., Rees, F., Sainte-Marie J., Salmon, E., Schiedung, M., Schimel, J., Wieder, W.,](#)  
 1185 [Abiven, S., Barre, P., Cecillon, L. and Guenet, B.: Soil organic carbon models need](#)  
 1186 [independent time-series validation for reliable prediction. \*Commun Earth Environ\*](#), 4, 158,  
 1187 <https://doi.org/10.1038/s43247-023-00830-5>, 2023.
- 1188 Lee, J., Viscarra Rossel, R. A., Zhang, M., Luo, Z. and Wang, Y. P.: Assessing the response of  
 1189 soil carbon in Australia to changing inputs and climate using a consistent modelling  
 1190 framework. *Biogeosciences*, 18, 5185-5202, <https://doi.org/10.5194/bg-18-5185-2021>, 2021.
- 1191 Lefèvre, C., Rekik, F., Alcantara, V. and Wiese, L.: Soil organic carbon: the hidden potential,  
 1192 Food and Agriculture Organization of the United Nations (FAO), [http://www.fao.org/3/a-](http://www.fao.org/3/a-i6937e.pdf)  
 1193 [i6937e.pdf](#), 2017.
- 1194 Lehmann, J. and Kleber, M.: The contentious nature of soil organic matter. *Nature*, 528, 60-68,  
 1195 <https://doi.org/10.1038/nature16069>, 2015.
- 1196 Liang, Z., Chen, S., Yang, Y., Zhou, Y. and Shi, Z.: High-resolution three-dimensional mapping  
 1197 of soil organic carbon in China: Effects of SoilGrids products on national modeling. *Sci Total*  
 1198 *Environ*, 685, 480-489, <https://doi.org/10.1016/j.scitotenv.2019.05.332>, 2019.

Deleted: Courier Corporation

Deleted: 1994

1201 Lorenz, K., Lal, R. and Ehlers, K.: Soil organic carbon stock as an indicator for monitoring land  
1202 and soil degradation in relation to United Nations' Sustainable Development Goals. *Land*  
1203 *Degrad Dev*, 30, 824-838, <https://doi.org/10.1002/ldr.3270>, 2019.

1204 Lunt, I. D., Eldridge, D. J., Morgan, J. W. and Witt, G. B.: A framework to predict the effects  
1205 of livestock grazing and grazing exclusion on conservation values in natural ecosystems in  
1206 Australia. *Australian Journal of Botany*, 55, 401-415, <https://doi.org/10.1071/BT06178>,  
1207 2007.

1208 Luo, Y., Ahlström, A., Allison, S. D., Batjes, N. H., Brovkin, V., Carvalhais, N., Chappell, A.,  
1209 Ciais, P., Davidson, E. A. and Finzi, A.: Toward more realistic projections of soil carbon  
1210 dynamics by Earth system models. *Global Biogeochem Cycles*, 30, 40-56,  
1211 <https://doi.org/10.1002/2015GB005239>, 2016.

1212 Luo, Z., Wang, E. and Sun, O. J.: Soil carbon change and its responses to agricultural practices  
1213 in Australian agro-ecosystems: a review and synthesis. *Geoderma*, 155, 211-223,  
1214 <https://doi.org/10.1016/j.geoderma.2009.12.012>. 2010.

1215 Marshall, T. J. and Holmes, J. W.: Soil physics, 2<sup>nd</sup> ed., Cambridge University Press, New York,  
1216 1988.

1217 McBratney, A. B., Santos, M. M. and Minasny, B.: On digital soil mapping. *Geoderma*, 117, 3-  
1218 52, [https://doi.org/10.1016/S0016-7061\(03\)00223-4](https://doi.org/10.1016/S0016-7061(03)00223-4), 2003.

1219 Minasny, B., McBratney, A. B., Malone, B. P. and Wheeler, I.: Digital mapping of soil carbon.  
1220 *Advances in agronomy*, 118, 1-47, <https://doi.org/10.1016/B978-0-12-405942-9.00001-3>,  
1221 2013.

1222 Mishra, U. and Riley, W.: Scaling impacts on environmental controls and spatial heterogeneity  
1223 of soil organic carbon stocks. *Biogeosciences*, 12, 3993-4004, <https://doi.org/10.5194/bg-12-3993-2015>, 2015.

1225 Mokany, K., Raison, R. J. and Prokushkin, A. S.: Critical analysis of root: shoot ratios in  
1226 terrestrial biomes. *Glob Change Biol*, 12, 84-96, <https://doi.org/10.1111/j.1365-2486.2005.001043.x>, 2006.

1228 Murphy, B. W.: Impact of soil organic matter on soil properties – a review with emphasis on  
1229 Australian soils. *Soil Research*, 53, 605-635, <https://doi.org/10.1071/SR14246>, 2015.

1230 Nyaupane, K., Mishra, U., Tao, F., Yeo, K., Riley, W. J., Hoffman, F. M. and Gautam, S.:  
1231 Observational benchmarks inform representation of soil organic carbon dynamics in land  
1232 surface models. *Biogeosci Discuss*, 2023, 1-28, <https://doi.org/10.5194/bg-2023-50>, 2023.

1233 Panchal, P., Preece, C., Penuelas, J. and Giri, J.: Soil carbon sequestration by root exudates.  
1234 *Trends Plant Sci*, 27, 749-757, <https://doi.org/10.1016/j.tplants.2022.04.009>, 2022.

1235 Poulter, B., MacBean, N., Hartley, A., Khlystova, I., Arino, O., Betts, R., Bontemps, S.,  
1236 Boettcher, M., Brockmann, C. and Defourny, P.: Plant functional type classification for earth  
1237 system models: results from the European Space Agency's Land Cover Climate Change  
1238 Initiative. *Geosci Model Dev*, 8, 2315-2328, <https://doi.org/10.5194/gmd-8-2315-2015>,  
1239 2015.

1240 Ren, C., Mo, F., Zhou, Z., Bastida, F., Delgado-Baquerizo, M., Wang, J., Zhang, X., Luo, Y.,  
1241 Griffis, T. J. and Han, X.: The global biogeography of soil priming effect intensity. *Global*  
1242 *Ecol Biogeogr*, 31, 1679-1687, <https://doi.org/10.1111/geb.13524>, 2022.

Deleted: Lobsey, C. and Viscarra Rossel, R.: Sensing of soil bulk density for more accurate carbon accounting. *Eur J Soil Sci*, 67, 504-513, <https://doi.org/10.1111/ejss.12355>, 2016.

Formatted: Superscript

1246 Rossel, R. V., Chen, C., Grundy, M., Searle, R., Clifford, D. and Campbell, P. The Australian  
1247 three-dimensional soil grid: Australia's contribution to the GlobalSoilMap project. *Soil Res*,  
1248 53, 845-864, <https://doi.org/10.1071/SR14366>, 2015.

1249 Rumpel, C., Amiraslani, F., Koutika, L.-S., Smith, P., Whitehead, D. and Wollenberg, E.: Put  
1250 more carbon in soils to meet Paris climate pledges, *Nature*, 564, 32-34,  
1251 <https://doi.org/10.1038/d41586-018-07587-4>, 2018.

1252 Six, J., Conant, R. T., Paul, E. A. and Paustian, K.: Stabilization mechanisms of soil organic  
1253 matter: Implications for C-saturation of soils. *Plant Soil*, 241, 155-176,  
1254 <https://doi.org/10.1023/A:1016125726789>, 2002.

1255 Smith, P.: Soil carbon sequestration and biochar as negative emission technologies. *Glob*  
1256 *Change Biol*, 22, 1315-1324, <https://doi.org/10.1111/gcb.13178>, 2016.

1257 Stockmann, U., Padarian, J., McBratney, A., Minasny, B., de Brogniez, D., Montanarella, L.,  
1258 Hong, S. Y., Rawlins, B. G. and Field, D. J.: Global soil organic carbon assessment. *Glob*  
1259 *Food Sec*, 6, 9-16, <https://doi.org/10.1016/j.gfs.2015.07.001>, 2015.

1260 Stockmann, U., Adams, M. A., Crawford, J. W., Field, D. J., Henakaarchchi, N., Jenkins, M.,  
1261 Minasny, B., McBratney, A. B., De Courcelles, V. d. R. and Singh, K.: The knowns, known  
1262 unknowns and unknowns of sequestration of soil organic carbon. *Agric Ecosyst Environ*,  
1263 164, 80-99, <https://doi.org/10.1016/j.agee.2012.10.001>, 2013.

1264 Terrer, C., Phillips, R. P., Hungate, B. A., Rosende, J., Pett-Ridge, J., Craig, M. E., van  
1265 Groenigen, K. J., Keenan, T. F., Sulman, B. N., Stocker, B. D., Reich, P. B., Pellegrini, A. F.  
1266 A., Pendall, E., Zhang, H., Evans, R. D., Carrillo, Y., Fisher, J. B., Van Sundert, K., Vicca, S.  
1267 and Jackson, R. B.: A trade-off between plant and soil carbon storage under elevated CO<sub>2</sub>.  
1268 *Nature*, 591, 599-603, <https://doi.org/10.1038/s41586-021-03306-8>, 2021.

1269 Todd-Brown, K., Randerson, J., Hopkins, F., Arora, V., Hajima, T., Jones, C., Shevliakova, E.,  
1270 Tjiputra, J., Volodin, E. and Wu, T.: Changes in soil organic carbon storage predicted by Earth  
1271 system models during the 21st century. *Biogeosciences*, 11, 2341-2356,  
1272 <https://doi.org/10.5194/bg-11-2341-2014>, 2014.

1273 Todd-Brown, K. E., Randerson, J. T., Post, W. M., Hoffman, F. M., Tarnocai, C., Schuur, E. A.  
1274 and Allison, S. D.: Causes of variation in soil carbon simulations from CMIP5 Earth system  
1275 models and comparison with observations. *Biogeosciences*, 10, 1717-1736,  
1276 <https://doi.org/10.5194/bg-10-1717-2013>, 2013.

1277 Viscarra Rossel, R. A., Webster, R., Bui, E. N. and Baldock, J. A.: Baseline map of organic  
1278 carbon in Australian soil to support national carbon accounting and monitoring under climate  
1279 change. *Glob Change Biol*, 20, 2953-2970, <https://doi.org/10.1111/gcb.12569>, 2014.

1280 Viscarra Rossel, R. A., Chen, C., Grundy, M. J., Searle, R., Clifford, D. and Campbell, P. H.:  
1281 The Australian three-dimensional soil grid: Australia's contribution to the GlobalSoilMap  
1282 project. *Soil Res*, 53, 845-864, <https://doi.org/10.1071/SR14366>, 2015.

1283 Viscarra Rossel, R. A., Lee, J., Behrens, T., Luo, Z., Baldock, J. and Richards, A.: Continental-  
1284 scale soil carbon composition and vulnerability modulated by regional environmental  
1285 controls. *Nat Geosci*, 12, 547-552, <https://doi.org/10.1038/s41561-019-0373-z>, 2019.

1286 Viscarra Rossel, R. A., Webster, R., Zhang M., Shen, Z., Dixon, K., Wang, Y. P., Walden, L.:  
1287 How much organic carbon could the soil store? The carbon sequestration potential of  
1288 Australian soil. *Glob Change Biol*, 30, e17053, <https://doi.org/10.1111/gcb.17053>, 2023.

1289 Wadoux, A. M. J., Román Dobarco, M., Malone, B., Minasny, B., McBratney, A. B. and Searle,  
1290 R.: Baseline high-resolution maps of organic carbon content in Australian soils. *Sci Data*, 10,  
1291 181, <https://doi.org/10.1038/s41597-023-02056-8>, 2023.

1292 Walden, L., Serrano, O., Zhang, M., Shen, Z., Sippo, J. Z., Bennett, L. T., Maher, D. T.,  
1293 Lovelock, C. E., Macreadie, P. I. and Gorham, C.: Multi-scale mapping of Australia's  
1294 terrestrial and blue carbon stocks and their continental and bioregional drivers. *Commun*  
1295 *Earth Environ*, 4, 189, <https://doi.org/10.1038/s43247-023-00838-x>, 2023.

1296 Wang, B., Waters, C., Orgill, S., Gray, J., Cowie, A., Clark, A. and Li Liu, D.: High resolution  
1297 mapping of soil organic carbon stocks using remote sensing variables in the semi-arid  
1298 rangelands of eastern Australia. *Sci Total Environ*, 630, 367-378,  
1299 <https://doi.org/10.1016/j.scitotenv.2018.02.204>, 2018a.

1300 Wang, B., Gray, J. M., Waters, C. M., Anwar, M. R., Orgill, S. E., Cowie, A. L., Feng, P. and Li  
1301 Liu, D.: Modelling and mapping soil organic carbon stocks under future climate change in  
1302 south-eastern Australia. *Geoderma*, 405, 115442,  
1303 <https://doi.org/10.1016/j.geoderma.2021.115442>, 2022.

1304 Wang, B., Waters, C., Orgill, S., Cowie, A., Clark, A., Li Liu, D., Simpson, M., McGowen, I.  
1305 and Sides, T.: Estimating soil organic carbon stocks using different modelling techniques in  
1306 the semi-arid rangelands of eastern Australia. *Ecol Indic*, 88, 425-438,  
1307 <https://doi.org/10.1016/j.ecolind.2018.01.049>, 2018b.

1308 Wang, Y. P., Zhang, H., Ciais, P., Goll, D., Huang, Y., Wood, J. D., Ollinger, S. V., Tang, X. and  
1309 Prescher, A. K.: Microbial activity and root carbon inputs are more important than soil carbon  
1310 diffusion in simulating soil carbon profiles. *J Geophys Res Biogeosci*, 126, e2020JG006205,  
1311 <https://doi.org/10.1029/2020JG006205>, 2021.

1312 Wieder, W., Grandy, A., Kallenbach, C., Taylor, P. and Bonan, G.: Representing life in the Earth  
1313 system with soil microbial functional traits in the MIMICS model. *Geosci Model Dev*, 8,  
1314 1789-1808, <https://doi.org/10.5194/gmd-8-1789-2015>, 2015.

1315 Wiesmeier, M., Barthold, F., Spörlein, P., Geuß, U., Hangen, E., Reischl, A., Schilling, B.,  
1316 Angst, G., von Lützw, M. and Kögel-Knabner, I.: Estimation of total organic carbon storage  
1317 and its driving factors in soils of Bavaria (southeast Germany). *Geoderma Regional*, 1, 67-  
1318 78, <https://doi.org/10.1016/j.geodrs.2014.09.001>, 2014.

1319 Wiesmeier, M., Urbanski, L., Hobbey, E., Lang, B., von Lützw, M., Marin-Spiotta, E., van  
1320 Wesemael, B., Rabot, E., Ließ, M. and Garcia-Franco, N.: Soil organic carbon storage as a  
1321 key function of soils-A review of drivers and indicators at various scales. *Geoderma*, 333,  
1322 149-162, <https://doi.org/10.1016/j.geoderma.2018.07.026>, 2019.

1323 Wynn, J. G., Bird, M. I., Vellen, L., Grand-Clement, E., Carter, J. and Berry, S. L.: Continental-  
1324 scale measurement of the soil organic carbon pool with climatic, edaphic, and biotic controls.  
1325 *Global Biogeochem Cycles*, 20, <https://doi.org/10.1029/2005GB002576>, 2006.

1326 Zhang, H., Goll, D. S., Wang, Y. P., Ciais, P., Wieder, W. R., Abramoff, R., Huang, Y., Guenet,  
1327 B., Prescher, A. K. and Viscarra Rossel, R. A.: Microbial dynamics and soil physicochemical

1328 properties explain large-scale variations in soil organic carbon. *Glob Change Biol*, 26, 2668-  
1329 2685, <https://doi.org/10.1111/gcb.14994>, 2020.

1330